2017

Turboelectric Distributed Propulsion System for NASA Next Generation Aircraft

Hashim H. Abada
Wright State University

TURBOELECTRIC DISTRIBUTED PROPULSION SYSTEM FOR NASA NEXT GENERATION AIRCRAFT

A thesis submitted in partial fulfillment of the

requirements for the degree of

Master of Science in Aerospace System Engineering

By

HASHIM H. ABADA

B.Sc. Mechanical Engineering, University of Al-Qadisiyah, 2013

2017

Wright State University

WRIGHT STATE UNIVERSITY
GRADUATE SCHOOL

December 4, 2017

I HEREBY RECOMMEND THAT THE THESIS PREPARED UNDER MY SUPERVISION BY Hashim H. Abada Entitled Turboelectric Distributed Propulsion System for NASA Next Generation Aircraft BE ACCEPTED IN PARTIAL FULFILLMENT OF THE REQUIREMENTS FOR THE DEGREE OF Master of Science in Aerospace System Engineering.

_____

Rory A. Roberts, Ph.D.
Thesis Director

_____

Joseph C. Slater, Ph.D., P.E.
Department Chair

Committee on Final Examination

_____

Rory A. Roberts, Ph.D.

_____

Zifeng Yang, Ph.D.

_____

Mitch Wolff, Ph.D.

_____

Barry Milligan, Ph.D.

Interim Dean of the Graduate School

ABSTRACT

ABADA, HASHIM H. M.S.A.S.E. Department of Mechanical and Materials Engineering, Wright State University, 2017. *Turboelectric Distributed Propulsion System for NASA Next Generation Aircraft.*

Next generation aircraft, more specifically NASA aircraft concepts, will include new technologies and make many advancements in fuel economy and noise. However, there are some challenges associated with the latest technologies that NASA is planning to use for the next generation aircraft. For example, these aircraft concepts require large amounts of electrical power to generate the required thrust throughout a notional flight profile. One of the new technologies is using advanced propulsion systems, such as the Turboelectric Distributed Propulsion (TeDP) system, which is significantly different from current aerospace high bypass turbofan based propulsion system. The TeDP propulsion system replaces the traditional turbofan engines with a series of embedded electrical fans. The blended wing body aircraft, N3-X (Boeing 777 class), that NASA proposed will have as many as 14 electric fans mounted on the upper aft surface of the aircraft wings. In addition to improved aircraft efficiency, this propulsion system change will significantly reduce noise generation, and provide the capability of short take-off and landing. A dynamic model of the ducted fan distributed propulsion system was developed and simulated for different notional flight profiles. The results show that the ducted fan distributed propulsion system dynamic model and the control system successfully

generate the required thrust for the flights and capture the transient behavior of the system throughout the flight profiles. In addition, the dynamic model was used to model a 50 passenger regional aircraft. This study shows the benefit of both the TeDP system and the flexibility of the developed model. The contribution to knowledge is the evolution of the evaluation model that helps researcher's understand propulsion systems such as the TeDP system of NASA N+3 class aircraft. By identifying and understanding the principal challenges and possibilities provided by the technology, this research further contributes to defining a roadmap of the new technology propulsion system for future research.

Table of Contents

List of Figures

List of Tables

Acknowledgements

Mainly, I would like to thank my thesis advisors, Dr. Rory Roberts and Dr. Mitch Wolff, for their guidance and support throughout this research. They are giving me an exciting opportunity to work on fantastic and vital thesis subject for NASA. By their guidance, I have learned a lot about the aircrafts especially the propulsion systems, I have gained a new experience about MATLAB/ Simulink software, and I have got new skills such as topic researching and choosing the appropriate courses skill regarding my thesis. They have worked with me as a friend and colleague, not a student, and their offices' door open for my questions and programming issues most of the time. Their support encouraged me to achieve my thesis goals that I may be wouldn't do without them.

Also, I would send big thanks to my father, mother, brothers, sisters, and friends for their efforts to support me with nostalgia words that helped me to calm my nostalgic feelings and their prayers that made the challenges of my life and research more accessible.

Additionally, I would like to thank my wife, daughter, and my son for their trust in me even in those stressful time, and for their efforts to make me successful in my life and study.

Finally, I would like to thank my sponsor Higher Committee for Education Development in Iraq (HCED) who helped and funded me to complete my Master's degree in the United States at Wright State University.

Nomenclature

Acronyms

AC	= Alternating Current
BLI	= Boundary Layer Ingestion
BPR	= Bypass Ratio
BWB	= Blended Wing Body
CAEP	= Committee on Aviation Environmental Protection
CESTOL	= Cruise Efficient Short Take-Off and Landing
DC	= Direct Current
FLC	= Fuzzy Logic Controller
FLOPS	= Flight Optimization System
FPR	= Fan Pressure Ratio
GRC	= NASA Glenn Research Center
HTS	= High Temperature Superconductive
HWB	= Hybrid-Wing-Body
IATA	= International Air Transport Association
IBF	= Internally Blown Flap
LQR	= Linear Quadratic Regulator
NPSS	= Numerical Propulsion System Simulator
PI Controllers	= Proportional-Integral Controller
RPM	= Revolution per Minutes
TeDP	= Turboelectric Distributed Propulsion
TSFC	= Thrust Specific Fuel Consumption
UHB	= Ultra-High Bypass ratio
USB	= Upper Surface Blowing
LH2	= Liquid Hydrogen

Symbols

A_{exit} = Nozzle Exit Area (m^2)

A_{Throat} = Nozzle Thorat Area (m^2)

a_{exit} = Exit speed of sound (m/s)

b_T = Total viscous friction (N.m.s)

b_m = Motor viscous friction (N.m.s)

b_L = Load viscous friction (N.m.s)

Cp = constant pressure specific heat

Friction Loss = Power Loss

I = Armature current

J = Loads moment of inertial

J_{Shaft} = Moment of inertia (combined Shaft, DC Motor, and Fan)

J_T = Total moment of inertia ($Kg.m^2$)

J_m = Motor moment of inertia ($Kg.m^2$)

J_L = Load moment of inertia ($Kg.m^2$)

$K\varphi$ = Electromagnetic field (emf) constant

L = Windings inductance

Mach = Mach number

$\dot{m}_{actual}$ = Actual mass flow rate

$\dot{m}_{normalized}$ = Normalized mass flow rate

$\dot{m}_2$ = Fan mass flow rate (Kg/s)

$\dot{m}_3$ = Nozzle inlet mass flow rate (Kg/s)

$\dot{m}_4$ = Nozzle exit mass flow rate (Kg/s)

N_{Design} = Design Fan Shaft Speed in r.p.m

$N_{normalized}$ = Normalize shaft speed

P = Power

P_1 & P4 = ambient pressure (Pa)

P_2 = Fan inlet total Pressure (Pa)

$P_{2design}$ = Design Fan inlet total Pressure (Pa)

P_3 = Nozzle inlet total Pressure (Pa)

P_{cr} = Outlet calculated Pressure of the critical pressure ratio (Pa)

$P_{critical}$ = Nozzle critical Pressure (Pa)

P_{exit} = Nozzle exit Pressure (Pa)

P_{Motor} = Power Supply from the DC Motor

Pr = pressure ratio

$Pr_{normalized}$ = Normalize pressure ratio

Pr $_{Design}$ = Design pressure ratio

P_{Losses} = Power Losses (KW)

$P_{Mechanical}$ = Mechanical Power (KW)

$P_{electrical}$ = Electrical Power (KW)

V_{exit} = Exit Velocity (m/s)

V = Voltage

V_1 = Inlet Velocity (m/s)

V_{mixer} = Mixer Volume

R = Gas constant

R = Windings resistance

R_{amb} = Ambient gas constant (J/mole. K)

RPM_{design} = Design rotational speed

RPM_{Shaft} = Operating Fan Shaft Speed in r.p.m

T = Torque

T_1 & T4 = Ambient Temperature (K)

T_2 = Fan inlet Temperature (K)

$T_{2design}$ = Design Fan inlet total Temperature (K)

T_3 = Nozzle inlet Temperature (K)

$T_{critical}$ = Nozzle critical Temperature (K)

T_{exit} = Nozzle exit Temperature (K)

W_{Fan} = Fan Work

W_{loss} = Shaft loss, Normalize, and Max Friction Loss

γ_{amb} = ambient specific heat ratio

$\zeta_{isentropic}$ = Isentropic Efficiency

ρ_{amb} = The ambient density of the air in (kg/sec)

Δh = change in enthalpy

ζ = DC Motor Efficiency

ω = Angular velocity (rad)

Ω = Ohm

1. Introduction

1.1. Project Overview

According to International Air Transport Association (IATA) passenger forecast, there were 2.8 billion air travel passengers worldwide in 2011 and the average annual increase in air travel passengers is projected to be 175 million annually to reach 3.5 billion air travel passengers in 2015[1]. This growth in the amount of air travel passengers will increase through future years. In addition, this growth will lead to many environmental and economic problems. In order to reduce and minimize the economic and environmental impacts due to the increase in air traffic, more electrical power systems will be used in the next generation of the civil aircraft technologies.

NASA has defined four ambitious goals targeting a decrease in emissions specifically NOx, fuel consumption, noise, and field length. These four ambitious goals are given in Table 1, where N+1, N+2, and N+3 represent different types of NASA next-generation aircraft. Meeting and achieving most of the N+1, N+2, and N+3 architectures requirements will require several technological concepts to be developed. The conventional tube and wing configurations have achieved the N+1 goals, while the Turboelectric Distributed Propulsion (TeDP) and Hybrid-Wing-Body (HWB) aircrafts have been suggested as a more suitable design to achieve the N+2 and N+3 goals[2].

Table 1: NASA N+3 Subsonic Fixed Wing Project Metrics[2]

CORNERS OF THE TRADE SPACE	N+1 (2015)*** Technology Benefits Relative to a Single Aisle Reference Configuration	N+2 (2020)*** Technology Benefits Relative to a Large Twin Aisle Reference Configuration	N+3 (2025)*** Technology Benefits
Noise (cum below Stage 4)	- 32 dB	- 42 dB	- 71 dB
LTO NOx Emissions (below CAEP 6)	-60%	-75%	better than -75%
Performance: Aircraft Fuel Burn	-33%**	-50%**	better than -70%
Performance: Field Length	-33%	-50%	exploit metroplex* concepts

*** Technology Readiness Level for key technologies = 4-6
** Additional gains may be possible through operational improvements
* Concepts that enable optimal use of runways at multiple airports within the metropolitan areas

A revolutionary change in the traditional engine and aircraft architecture is required to achieve these strict and challenging goals. The revolutionary change in traditional engine design can be achieved by increasing the overall efficiencies (adiabatic and propulsive efficiency) of the engine[3]. The propulsive efficiency can be increased by increasing the Bypass Ratio (BPR). In addition, increasing the BPR reduces the level of the fuel required. For instance, an increase in the BPR causes a decrease in the Thrust Specific Fuel Consumption (TSFC), but there are limits to how much the BPR can be increased. However, with the continuous increase in BPR, the total pressure losses of the fan will rise due to the continuous decrease of the Fan Pressure Ratio (FPR). The total pressure

losses of the fan rose, because of the increase of the inlet fan diameter required to counter-balance the benefits of increasing the BPR.

The TeDP system on a Hybrid Wing Body (HWB) aircraft is considered a revolutionary technique to circumvent these issues by giving a high effective bypass ratio and more suitable design to achieve the N+3 stringent goals [4].

1.2. Scope

The scope of this thesis focuses on the propulsion system architecture of the next generation aircraft of a conceptual aircraft using a TeDP system on a Blended Wing Body airframe. NASA's N3-X is considered an excellent example of a next generation aircraft, and it is expected to be in service in the 2030-2035 time frame as shown in Figure 1.

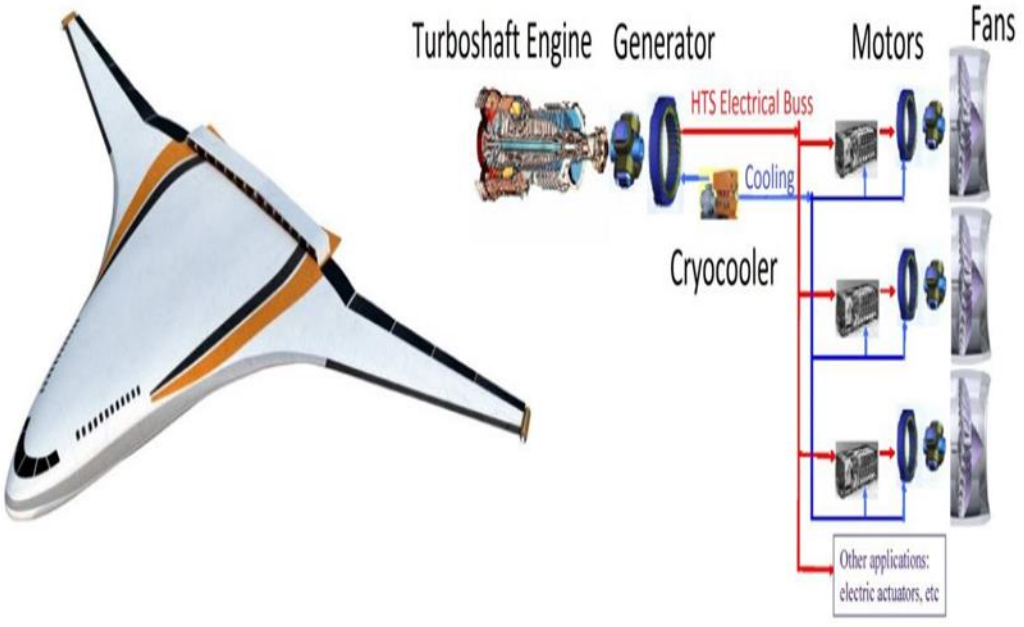

Figure 1: NASA's N3-X Aircraft with a Turboelectric Distributed Propulsion System [3]

The main components of NASA's N3-X aircraft consist of two turbo generators, fourteen electrical ducted fans, a cryogenic refrigeration system, and inverters. Specifically, the two turbo generators consist of two turboshaft engines, which are mounted on the wingtips, driving two high-speed, High Temperature Superconductive (HTS) generators, which supply adequate electrical power for primary and secondary use. The HTS generators are considered the primary electrical power supply in the N3-X aircraft. The primary electrical use component is the fourteen electrical ducted fans, which consist of a fan, HTS motor, shaft, mixer volume, and a nozzle. The fourteen electrical ducted fans are the propulsion system in the N3-X aircraft (i.e., the only source of the aircraft thrust), and they are embedded into the upper aft surface of the aircraft wing airframe. The N3-X aircraft cooling system which is a cryogenic refrigeration system is vital. It is a fundamental component that is used to reduce the heat energy and to cool down essential N3-X aircraft components such as HTS fan motors, HTS generators, inverters, transmission lines, and others. The secondary use components are all the regular aircraft parts, which need electricity, such as lights, and kitchen, etc.

The TeDP system has two main parts: (1) the electrical power supply which is a turbo-generator (2) the propulsion system which consists of electrical ducted fans. The (TeDP) system has many benefits for this aircraft[5]. First, it increases the propulsive efficiency by reducing the propulsion system weight (replacing the large single turbofan engine with fourteen smaller electrical ducted fans). Second, it uses power transmission technology with a high efficiency (i.e. HTS generators, motors, and transmission lines). Third, the electrical transmission lines that connect the propulsion system (fourteen ducted fans) with the two turbo-generators replace a gearbox with a variable gear ratio. That means

the turbine shaft speed inside the turbo-generator, and the ducted fan shaft speed are run at their optimum speed independently. In other words, the turbine shaft and fan shaft speeds work independently of one another[6]. In addition, the two turbo-generators make less noise compared to the traditional aircraft. That is because the turbo-generators only produce electricity without thrust. Another benefit is that this aircraft produces less noise because forward and aft of the ducted fans is shielded by the airframe and the velocity of the core exhaust of the ducted fans and the turbo-generators are much lower than a traditional turbofan jet engine which produces thrust. In addition, the aircraft has very low emissions because it uses Liquid Hydrogen (LH2) as a fuel. LH2 burns cleaner and less fuel is needed compared the Jet-A fuel need for a turbofan engine. Moreover, turbomachinery efficiency is higher due to the smaller diameter size of the turbo-generator, since there is no fan in the core of the turbo-generator. Finally, because there are multiple fans used to produce thrust, NASA's N3-X is considered to be a more safe and reliable system especially if a failure happens to one of the fourteen fans compared to a traditional aircraft with just two engines and then losses one. A Boeing 777-200LR is used as a baseline aircraft to establish NASA's N3-X performance [7].

1.3. Objectives

The primary objective of this research is to examine and explore NASA's next generation aircraft N+3 architecture. More specifically, the turboelectric distributed propulsion system in conjunction with a Hybrid-Wing-Body (HWB) airframe. Therefore, the main goal of this thesis is to create an appropriate dynamic mathematical model of the distributed propulsion system that meets N+3 architecture requirements by using NASA's N3-X aircraft as the aircraft.

The tasks of this thesis are:

1. Develop a methodology to analyze the distributed propulsion system.
2. Develop a dynamic mathematical model to calculate the thrust (including parametric studies).
3. Comparing the dynamic mathematical model results with Cranfield University's results (i.e., NASA results).
4. Demonstrating the flexibility of the propulsion system model by examining a weather related flight.
5. Utilizing the scalability of the propulsion system model to design a regional transport aircraft distributed propulsion system.

2. Background

2.1. NASA Concepts

NASA has created many different conceptual ideas to achieve its four ambitious goals starting from N+1, N+2, and N+3 goals by interacting with many universities such as Cranfield University, and companies like Boeing aerospace, Ball Aerospace and Technology, and Airbus, etc.

2.1.1. NASA N+1 Concepts

In 2009[8], NASA utilized a conventional aircraft tube body, wings, and tail namely a subsonic fixed wing aircraft to achieve the N+1 goals. NASA proposed some improvements on the Boeing 737-800 airplane with General Electric CFM56-7B engines to meet N+1 goals, which are a reduction in fuel burn by 33%, reduction in oxides of nitrogen produced by 60% (set by the Committee on Aviation Environmental Protection [CAEP] in 2004), and a reduced take-off airfield length. Many improvements were proposed on the Boeing 737-800/CFM56-7B aircraft to transform it into a conceptual N+1 airplane. First, modifying the CFM56-7B turbofan by introducing an Ultra-High Bypass ratio (UHB) propulsion system combined with a novel noise reduction technology (3IB Chevron Coannular Nozzle configuration). Second, modulating the wings architecture design by increasing the wing sweep and adding winglets in order to reduce: the time, which is needed to create lift; and the effects of induced drag. These reductions lead to an airplane with an efficient fuel burn system, due to less fuel needed to create lift. Because of the less fuel needed, lower emissions are produced such as CO_2.

Another proposed improvement is increasing the desired cruise Mach number from 0.785 to 0.8 to get a higher airspeed. These improvements would result in rising the range of the Boeing 737-800 airplane from 3060 nm to 3250 nm. Additional improvements are proposed by using light composite construction materials for the fuselage, wing, and tail assembly resulting in a 15% weight reduction. Finally, improving the hydraulic pressure system by increasing the pressure to 5000 psi has been proposed.

There are many similarities between the Boeing 737-800/CFM56-7B aircraft and the NASA conceptual N+1 aircraft. Both have an equal number of passengers, which is 162; one aisle; the same cabin configuration; and two-class seating. Also, the taper and aspect ratio of the wing is similar. The conceptual N+1 airplane schematic is shown in Figure 2.

Figure 2: Conceptual N+1 airplane schematic [5]

2.1.2. NASA N+2 Concepts

In 2006[9], NASA explored a new technology of airplanes and propulsion concepts for achieving N+2 goals in collaboration with Boeing Phantom Works. One proposed N+2

airplane is a Cruise Efficient Short Take-Off and Landing (CESTOL) airplane, shown in Figure 3.

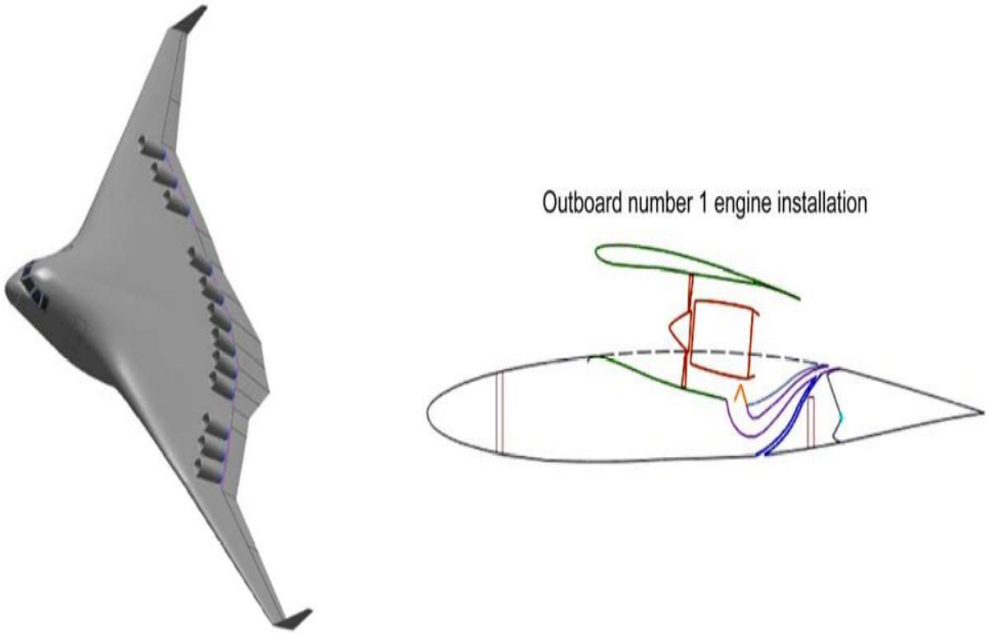

Figure 3: N+2 aircraft Cruise Efficient Short Take-off and Landing (CESTOL) [7]

The CESTOL aircraft is a combination of the Blended Wing Body (BWB) and the embedded distributed propulsion system. The BWB airframe type has been chosen because of its many benefits. For example, quiet aircraft operation, high cruise efficiency, and a huge internal volume for implementing an embedded distributed propulsion system. In addition, the designers chose the Internally Blown Flap (IBF) system, which is considered one of the most efficient powered lift systems. The distributed propulsion system consists of 12 small engines with low pressure fan bypass; these 12 small engines reroute cold air and are subsonic in order to lower the powered lift system noise. Six of these engines are embedded within the wings architecture and mounted along the wing upper aft surface.

NASA Glenn Research Center (GRC) used a Numerical Propulsion System Simulator (NPSS) model to estimate the performance of the engines. In addition, GRC suggested using engines with a very high BPR of 9.4. They also recommended the performance of individual engine components (a fan with a maximum pressure ratio of 2, a high pressure compressor with a pressure ratio of 20 and polytrophic efficiency of 91%, a low and high pressure turbine with a polytrophic efficiency of 93%, and a nozzle with a variable area. The CESTOL aircraft is therefore characterized by having a short takeoff and landing requirement, in addition the low noise, through these design changes.

2.1.3. NASA N+3 Concepts

In 2011[10], the N3-X aircraft is considered the conceptual aircraft that achieves the N+3 goal, as shown in Figure 4. The CESTOL aircraft is deemed the baseline of the N3-X aircraft. However, NASA proposes the use of a new technology of propulsion system in the N3-X aircraft, which is the Turboelectric Distributed Propulsion System (TeDP). Also, they depend on the Upper Surface Blowing (USB) system for creating powered lift, instead of using the Internally Blown Flap, because the structure and mechanical design of the USB system is more efficient. As a result, the N3-X aircraft configuration is a Hybrid Wing Body (HWB) aircraft, integrated with the TeDP system.

The N3-X aircraft's propulsion system is different from the CESTOL aircraft's propulsion system, which used 12 small engines. The TeDP system has 14 electrical fans driven by superconducting motors. These electrical fans are protected by a continuous nacelle embedded into the upper aft surface of the aircraft wing airframe. The 14 electric fans are powered by two turboshaft superconducting generators located at the wing tips through superconducting transmission electrical lines[11]. In addition, NASA researchers

proposed using superconducting materials for the electric components because the electrical resistance losses can be neglected (i.e., the electrical losses are almost zero) and high electrical current in small wires which are very compact and light can be used. Nevertheless, these materials need to be cooled to under the critical temperature, for this reason, they decided to use a cryogenic system.

The BWB airframe type was chosen because of its benefits which are a high lift-to-drag ratio, a decreased fuel burn (due to boundary layer ingestion over the aircraft fuselage), and low noise by shielding the distributed electric fans with the airframe.

Figure 4: A BWB N+3 Turboelectric Distributed Propulsion Aircraft [10]

3. Methodology

The traditional technology of an airplane's propulsion system is based on gas turbines such as jet, turboprop, and turbofan engines. The jet aircraft propulsion system is based on a jet engine, which is a gas turbine engine. The most common advanced engines used today are turbofan engines with a bypass duct, such as the GE 90 and GE115B turbofan engines. The GE 90 through the GE115B turbofan engines generate the on-board electric power and total thrust of the airplane. In addition, the GE 90 through the GE115B turbofan engines are producing the total thrust in two ways. The primary thrust, which is generated through the engine core (i.e., through the compressor, combustor, and turbine to the nozzle), and the secondary thrust is generated through the high bypass ratio duct to the nozzle. Both utilize a fan located at the front of the turbofan engine which withdraws air from the front of the airplane into the engine. The fuel is burned in the engine core section and when exhausted to the turbine generates the work required to drive both spools in order compress the incoming air. The by-pass generates thrust from passing a high mass flow rate of air by using a low shaft speed that withdraws the airstream through the bypass duct. As a result, the GE 90 through the GE115B turbofan engines produces ~40% of the total thrust from the bypass flow [12].

The N3-X aircraft propulsion system is based on 14 small electrical ducted fans using the high bypass ratio concept, the turbofan by-pass air stream, to generate thrust. As a result, generating thrust without using the engine core: compressor, combustor, and turbine.

However, these 14 electric ducted fans are driven by superconducting motors. The superconducting motors are powered from two superconducting generators located at the wing tips through superconducting transmission lines. That means the N3-X aircraft separates the generation of the total thrust and electrical power on the aircraft. This separation is a crucial benefit because the turbine shaft speed into the turbo-generator and the fan shaft speed can be operated at its optimum speed independently. In other words, the turbine shaft and fan shaft speed operate independently of each other [6]. A comparison between a turbofan engine and an electrical ducted fan is shown in Figure 5.

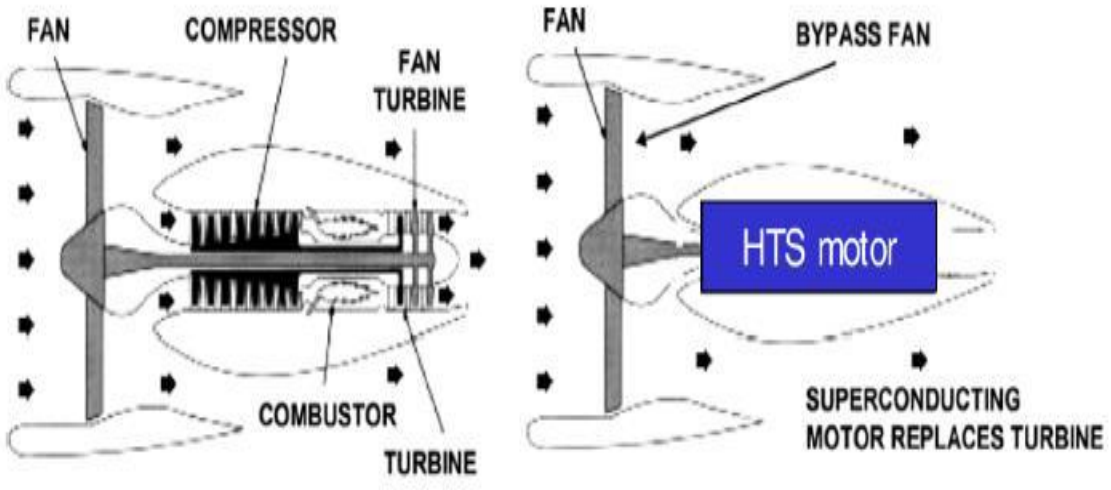

Figure 5: Turbofan vs. Electrical Fan [13]

This section contains the design of the distributed propulsion system for the conceptual N3-X aircraft, and a brief description about the inputs, calculations, and functions of each component, as well as the basic equations used to create the physics based mathematical model. The MATLAB/Simulink mathematical model of the propulsion system is shown in Figure 6. The various system components have been represented as blocks in the MATLAB/Simulink model. These components, or blocks, are flight profile, environment,

electric motor, fan shaft speed, fan, nozzle, plenum volume, and other subsystems and control blocks.

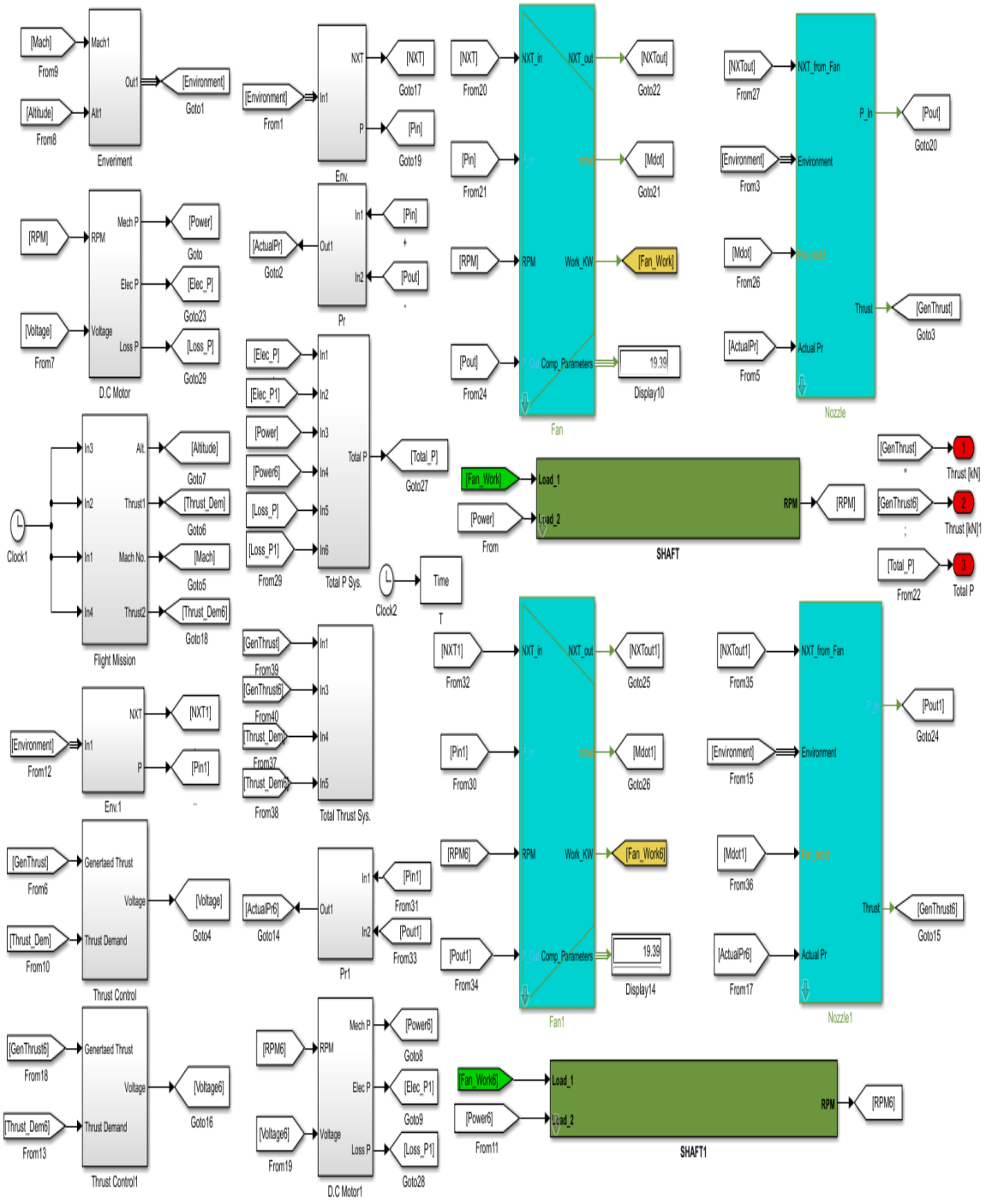

Figure 6: NASA N3-X Propulsion System Ducted Fan Simulink Model

3.1 Flight Profile

The flight profile subsystem contains flight data of the aircraft. More specifically, this subsystem consists of three lookup tables, which are Mach number, altitude, and demanded thrust with time, which is the only input for this subsystem. Also, the numbers, or values, which have been substituted into these lookup tables are set out using vectors and can be changed quickly to make a different or new flight profile (i.e., dynamic flight data). The Mach number and altitude lookup tables have been inserted into the environment block, and the thrust demand lookup table has been inserted into the control system block. As a result, the flight profile subsystem sets the boundary conditions.

3.2 Environment

The environment subsystem block is important to the propulsion system Simulink model. The environment parameters are calculated depending on the two main input parameters which are the Mach number and altitude. Mach number and altitude data are combined using a bus signal in the Simulink model to create the environment air properties subsystem. The ambient pressure, temperature, dynamic viscosity, and thermal conductivity are estimated via interpolation-extrapolation lookup tables with vector values dependent on the altitude by using U.S. Standard Atmosphere Air Properties. Also, gamma interpolation-extrapolation lookup table's vector values are created depending on the ambient temperature vector values. Air density values are calculated by using the ideal gas law for dry air; speed of sound values are calculated depending on gamma, gas constant, and ambient temperature values; total temperature values are estimated relying on Mach number, gamma, and ambient temperature values; total pressure values are estimated depending on the total temperature, the ambient pressure,

the static temperature, and gamma values; and total air density values are calculated relying on gamma, total temperature, air density, and ambient temperature values. The composition of air is considered one of the inputs into the model, the composition of air by mole is assumed as shown in Table 2. All of the interpolation-extrapolation lookup tables and input parameters are combined using a bus signal to create the atmospheric data.

Table 2: Composition of Air by Mole Fraction [14]

Constituent	Chemical Symbol	Molar Fraction
Oxygen	O2	0.21
Nitrogen	N2	0.79
Methane	CH4	0.0
Hydrogen	H2	0.0
Carbon Dioxide	CO2	0.0
Carbon Monoxide	CO	0.0
Water Vapor	H2O	0.0

3.3 Electric Motor

Two turbo-generators, which are mounted on the wingtips, are supplying power to the high speed High Temperature Superconductive (HTS) generators which provides electrical power to the propulsion system of fourteen HTS motors. The two turboshafts produce the shaft power which is converted to electrical AC power by the two generators;

a rectifier converts the electrical AC power to DC power which is transferred through cryogenic lines to the electrical HTS motor as shown in Figure 7.

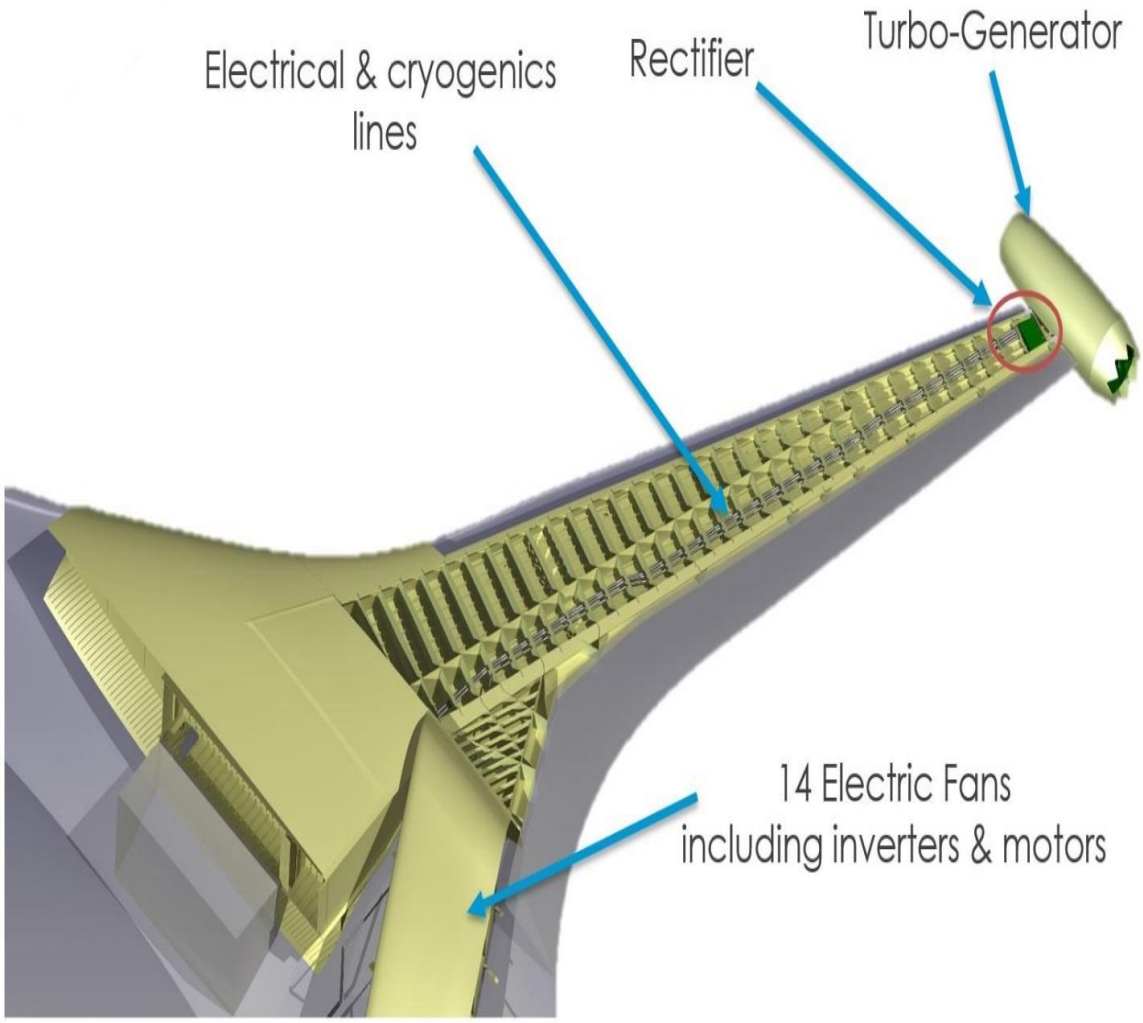

Figure 7: Electrical Power Distribution for N3-X Aircraft [15]

The high temperature superconducting materials are used for the electric motors rather than the traditional induction motors. The main reason is the weight of the conventional motors, which are incapable of achieving the required power to weight ratio needed for the N3-X aircraft. The weight of the HTS electric motors is less than the conventional induction motors by 30%. In addition, the volume and the total load losses of the HTS

electric motors are less than the conventional induction motors by 50% and 40%, respectively. Reducing the temperature of the superconducting wires of the electric motors drives the electrical resistance to almost zero. Therefore, it can carry high load electricity (voltage or current) in small wires, and use compact motors resulting in higher power density and efficiency [2].

The electrical motor used in the propulsion system Simulink model is assumed to be an electrical DC motor since the latest generation of the HTS taping and wiring does not exist. The electrical DC motor model consists of an inductance, internal resistance, and magnet, and it produces a torque on the shaft driving the fan. The inputs to the electric motor are the voltage source, V, and ω, which used to calculate RPM. The output is the mechanical and electrical power which are deemed the primary output and the heat losses, P_{Losses},. The value of the input voltage varies with time depending on the thrust generated and demanded, which is governed by the control system. The initial voltage value is set equal to 100 V. Also, ω varies with time depending on the shaft governing equations in the following section.

The equations used to create the electrical motor are conservation of energy using Kirchhoff's voltage law:

$$\frac{di}{dt} = \frac{V}{L} - \frac{R}{L} I - \frac{K_{\emptyset}}{L} \omega \qquad (1)$$

The physical parameters values of the electric motor are [16]:

L = 0.1 H

Kφ = 0.003 V/rad/sec

J_m = 0.1 Kg.m^2

b_m = 0.01 N.m.s

R = 0.4 Ω

The electric motor produces a torque, T, which is proportionate to the electromagnetic field or the strength of the magnetic field, Kφ, and the armature current, I,. The output mechanical power $P_{Mechanical}$ generated by the electric motor, which is calculated by multiplying the torque T with the angular velocity ω as shown in Equation (2).

$$P_{Mechanical} = T\omega = \mathrm{K}_{\varphi}\mathrm{I}\omega \tag{2}$$

The electrical power $P_{electrical}$ is calculated by multiplying the voltage V with the armature current I as shown in Equation (3), and this power is the total power of the electrical DC motor. The second output, which is the power losses P_{Losses}, is calculated by using equation (4) which is subtracting the mechanical power $P_{Mechanical}$ from the total electrical power. There are some methods to calculate the efficiency ζ of the DC motor. The easiest way is through the power types because they have already estimated. As a result, Equation (5) is used to calculate the efficiency ζ which is the ratio of the motor mechanical or net power to the total electrical power. The output mechanical power $P_{electrical}$ represents the only source of power that the propulsion system receives.

$$P_{electrical} = V.I \tag{3}$$

$$P_{Losses} = P_{electrical} - P_{Mechanical} \tag{4}$$

$$\zeta = \frac{P_{Mechanical}}{P_{electrical}} * 100\% \quad (5)$$

3.4 Shaft

The shaft connects the fan and the electric DC motor. Specifically, the shaft transfers the power from the electric DC motor to the fan. There are three inputs to the shaft subsystem: the load input signals are the mechanical load of the fan, the DC motor mechanical power, and the power disapated by friction losses. There is one output of the shaft, which is the angular velocity ω (i.e., fan shaft speed), and it is used as a feedback input to the DC motor. The DC motor power supply load signal represents the positive power load, and the power extracted from the fan load signal represents the negative or reaction load. The power friction losses $P_{friction}$ represents the bearing losses (viscous friction) of the motor and shaft. The governing equation (6) is used to calculate the angular velocity. The moment of inertia of the entire assembly is represented by *J*. The sum of the torques on the shaft are used to track the rotational energy.

$$\frac{d\omega}{dt} = \frac{P_{motor} + P_{Fan} + P_{friction}}{J * \omega} \quad (6)$$

Where

$$P_{friction} = A\omega^2 \quad (7)$$

3.5 Fan

The main component of the propulsion system Simulink model is the fan subsystem block. The fan function is considered a low pressure compressor which is located at the front of the ducted fan and responsible for withdrawing air into the duct or plenum volume, and it is driven by a shaft. The ducted fan architecture model is pictorial with flow station numbering in Figure 8. There are four input variables, which are shaft speed, RPM, total pressure, P_2, air properties, and outlet pressure, P_3, and four output variables, which are mass flow rate, $\dot{m}_2$, temperature, T_3, fan power, P_{Fan}, and air properties. Many different equations are used to calculate the output variables within the fan subsystem model. The fan map is explained in the Appendix below.

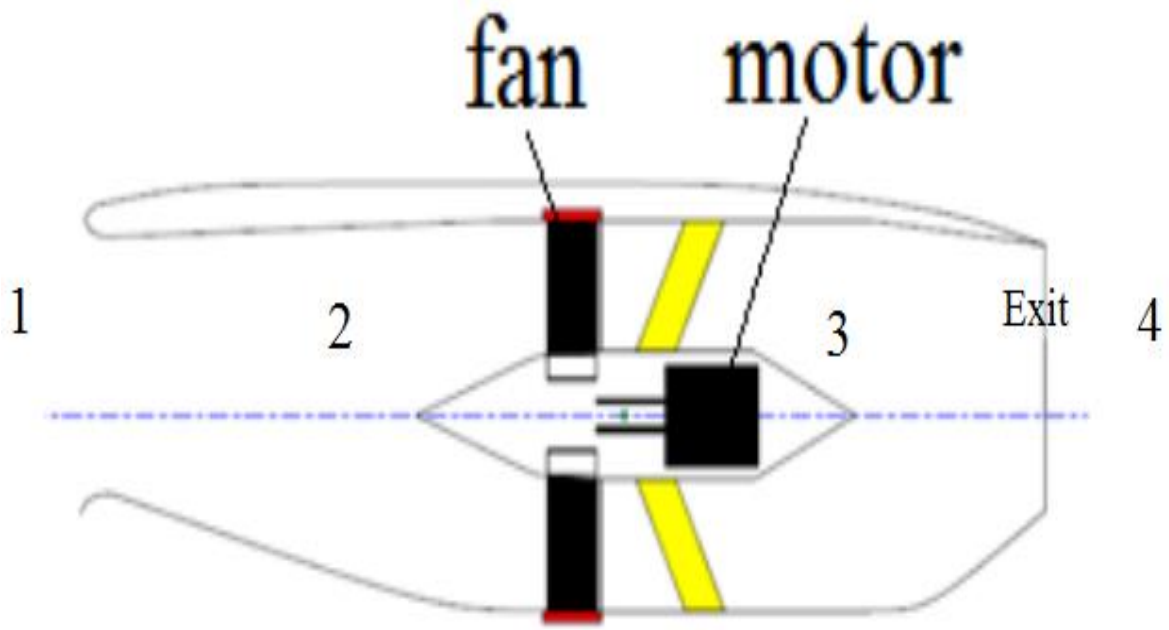

Figure 8: NASA N3-X Ducted Fan Propulsion System Architecture

3.5.1 Inlet Variables

The input parameters include molar composition of the flow, flow inlet temperature T_2, pressure inlet and pressure outlet. The fan outlet pressure is calculated within the mixer volume or bypass plenum volume. A brief explanation of this term will be discussed in the mixer volume component within the nozzle subsystem block. The total pressure at the front of the propulsion system is calculated assuming no heat loses as shown below:

$$P_2 = P_1 + \frac{1}{2} * \rho_1 * (Mach * \sqrt{\gamma_1 * R_1 * T_1})^2 \quad (8)$$

The parameters vary with time step depending on the altitude and Mach number of the aircraft, and the variables are estimated within the Environment subsystem block.

3.5.2 Output Variables

3.5.2.1 Mass Flow Rate

The outlet mass flow rate is based on the inlet pressure, inlet temperature, design mass flow rate, design inlet pressure, design inlet temperature, and normalized mass flow rate values. A performance map has been designed within the fan subsystem block to calculate the normalized mass flow rate that depends on the design and correct mass flow rate for given input values which are pressure ratio and rotational speed. The performance map is represented by a 2D interpolation lookup table using the normalized pressure ratio values $Pr_{normalized}$ and the normalize shaft speed values $N_{normalized}$ as inputs. The normalize pressure ratio values are based on the inlet and outlet pressure and the design pressure ratio Pr_{design}, and the normalize shaft speed values are depending on the inlet and design

temperature $T_{2design}$ and the inlet and design rotational speed RPM_{design}. Equation (9) and (10) are used to calculate the normalize shaft speed and pressure ratio.

$$Pr_{normalized} = \frac{P_3}{P_2 * Pr_{design}} \tag{9}$$

$$N_{normalized} = \left(\frac{RPM}{\sqrt{T_2}}\right) * \left(\frac{\sqrt{T_{2_{design}}}}{RPM_{design}}\right) \tag{10}$$

The normalized mass flow rate $\dot{m}_{normalized}$ are estimated by interpolating the two normalized inputs within the matrix that is established in advance. The output mass flow rate $\dot{m}_2$ are calculated after estimating the normalized mass flow rate. For steady flow, the nozzle inlet mass flow rate $\dot{m}_3$ is equal to the outlet mass flow rate of the fan $\dot{m}_2$. Equation (11) is used to calculate the output mass flow rate of the fan.

$$\dot{m}_2 = \dot{m}_3 = \dot{m}_{normalized} * \left(\frac{\dot{m}_{design} * \sqrt{T_{2_{design}}}}{P_{2_{design}}}\right) * \frac{P_2}{\sqrt{T_2}} \tag{11}$$

3.5.2.2 Outlet Temperature

The outlet temperature is based on the inlet pressure, inlet temperature, outlet pressure, heat specific ratio, and isentropic efficiency values. A performance map has been designed within the fan subsystem block to calculate the isentropic efficiency, $\zeta_{isentropic}$, for given input values, which are normalized pressure ratio and rotational

speed. The specific heat ratio γ is based on the constant pressure specific heat Cp and gas constant R. The constant pressure specific heat Cp values are calculated from the sum of multiplying the constant pressure specific heat as a function of outlet design temperature with the molar composition of the air stream flow. Equation (12) is used to estimate the specific heat ratio. Finally, the outlet temperature T_3 is calculated after estimating these parameters especially the isentropic efficiency as shown in equation (13).

$$\gamma = \frac{C_p}{C_p - R} \tag{12}$$

$$T_3 = T_2 * \left[1 + \frac{\left(\frac{P_3}{P_2}\right)^{\left(\frac{\gamma-1}{\gamma}\right)} - 1}{\zeta_{isentropic}} \right] \tag{13}$$

3.5.2.3 Fan Power

The power extracted from the fan subsystem block represents the negative or reaction power as predicated based on the inlet and outlet enthalpy, and the actual or outlet mass flow rates. The inlet and outlet enthalpy depend on the inlet and outlet temperature, the molar composition of the air stream flow, and the constant pressure specific heat Cp. The change in enthalpy values is calculated from multiplying the molar composition of the airstream flow with the ratio of the third order fit for the constant pressure specific heat Cp for air component gases with inlet and outlet temperature to the molar mass of the air component gases. Equation (14) is used to estimate the change in enthalpy. Finally, the

power extracted from the fan P_{Fan} is calculated by multiplying the change in enthalpy Δh with the outlet mass flow rate $\dot{m}_2$ as shown in the equation (15).

$$\Delta h = C_P * (T_3 - T_2) \tag{14}$$

$$P_{Fan} = \dot{m}_2 * \Delta h \tag{15}$$

3.6 Nozzle

The second component of the propulsion system Simulink model is the nozzle subsystem block. The nozzle is considered the rear part of the ducted fan, and it is a convergent variable area nozzle. The airstream flow is coming from the fan entering the mixer volume block then entering the nozzle. The nozzle is responsible for creating the required thrust needed to drive the aircraft forward. There are four input variables which are the ambient pressure P_1 and velocity V_1, air properties, actual pressure ratio Pr, and actual or mass flow rate $\dot{m}_3$, and two output variables which are the required thrust of the aircraft and inlet pressure to the mixer volume pressure P_3. There are many different equations and subsystem blocks are used to calculate the output variables within the nozzle subsystem model.

3.6.1 Plenum Volume

The inlet pressure to the mixer or plenum volume pressure P_3 is based on the inlet and outlet mass flow rate, the nozzle inlet temperature, the mixer or plenum volume, and the gas constant R. For steady flow, the plenum inlet mass flow rate $\dot{m}_3$ is equal to the outlet mass flow rate of the fan $\dot{m}_2$. According to the conservation of mass, the outlet mass flow rate of the mixer volume is equal to the exit mass flow rate of the nozzle $\dot{m}_4$ during

steady flow. The gas constant R is estimated from the ratio of the universal gas constant to the average molar mass. The inlet pressure P_3 is calculated from integration the ideal gas law with the time, equation (16), and the advantage of this equation is removed the algebraic restrictions. Also, the dynamic of mixer volume allows unsteady flow in the plenum volume between the fan and nozzle. The difference in the mass flow rate will result in a change in the plenum volume pressure P_3 that will dynamically drive the difference in the mass flow rate to zero.

$$P_3 = \int \frac{(\dot{m}_3 - \dot{m}_4) * R * T_3}{V_{mixer}} dt \tag{16}$$

3.6.2 Critical Pressure Ratio subsystem

The critical pressure ratio subsystem block depends on the inlet pressure P_3 and the specific heat ratio γ to calculate the critical pressure ratio. Because of the type of nozzle, a convergent variable nozzle, there are several steps used to determine the exit pressure and velocity required to calculate the thrust. The foremost step is to calculate the critical pressure ratio to compare with the nozzle actual or ambient pressure ratio.

The comparison will determine whether the nozzle flow is choked or nonchoked flow. Equation (17) is used to calculate the critical pressure ratio.

$$\left(\frac{P_{cr}}{P_3}\right)_{critical} = \left(\frac{2}{\gamma + 1}\right)^{\left(\frac{\gamma}{\gamma - 1}\right)} \tag{17}$$

There are two prospective cases, the flow of the nozzle is choked or nonchoked flow determined by calculating the nozzle actual or ambient pressure ratio $\left(\frac{P_4}{P_3}\right)_{actual}$ and comparing with critical pressure ratio $\left(\frac{P_{cr}}{P_3}\right)_{critical}$. Equations (18) and (19) are used to determine the nozzle flow type.

$$\left(\frac{P_{cr}}{P_3}\right)_{critical} \gg \left(\frac{P_4}{P_3}\right)_{actual} = Chocked\ Flow \tag{18}$$

$$\left(\frac{P_{cr}}{P_3}\right)_{critical} \ll \left(\frac{P_4}{P_3}\right)_{actual} = Nonchocked\ Flow \tag{19}$$

3.6.3 Nozzle Choked Flow Case

The exit pressure, velocity, and mass flow rate of the outlet flow required to estimate the required thrust can be calculated after the equations or critical pressure ratio subsystem determines the flow is choked flow.

Equation (20)[14] is used to calculate the mass flow rate exiting the nozzle $\dot{m}_4$ based on the mixer volume inlet pressure and temperature, specific heat ratio, throat area, and the gas constant.

$$\dot{m}_4 = P_3 * A_{Throat} * \sqrt{\frac{\gamma}{R * T_3}\left(\frac{2}{\gamma+1}\right)^{\left(\frac{\gamma}{2(\gamma-1)}\right)}} \tag{20}$$

The nozzle exit pressure P_{exit} for the choked flow is equal to the critical pressure $P_{critical}$. The critical pressure $P_{critical}$ is based on the nozzle inlet or mixer pressure and the specific heat ratio γ. Equation (21) is used to calculate the exit pressure P_{exit}.

$$P_{exit} = P_{critical} = P_3 * \left(\frac{2}{\gamma + 1}\right)^{\left(\frac{\gamma}{\gamma - 1}\right)} \tag{21}$$

The exit velocity depends on the exit Mach number, exit temperature, exit speed of sound, gas constant R, and specific heat ratio γ. For choked flow, the exit Mach number is equal to 1 as shown in equation (22). The exit temperature T_{exit} is depend on the specific heat ratio γ and the nozzle inlet temperature T_3 as shown in equation (23). The exit speed of sound a_{exit} is based on the exit temperature T_{exit}, gas constant R, and specific heat ratio γ as shown in equation (24). Finally, after calculating these parameters, the exit velocity V_{exit} of the nozzle is estimated by multiplying the exit Mach number with the exit speed of sound, equation (25).

$$Mach_{exit} = 1 \tag{22}$$

$$T_{exit} = T_{critical} = T_3 * \left(\frac{2}{\gamma + 1}\right) \tag{23}$$

$$a_{exit} = \sqrt{\gamma * R * T_{exit}} \tag{24}$$

$$V_{exit} = Mach_{exit} * a_{exit} \tag{25}$$

3.6.4 Nozzle Non-Choked Flow Case

The exit pressure, velocity, and mass flow rate of the outlet flow needed to estimate the required thrust can be calculated after critical pressure ratio subsystem determines the flow is nonchoked.

The nozzle exit pressure P_{exit} for nonchoked flow is equal to the ambient pressure P_4, Equation (26).

$$P_{exit} = P_4 \tag{26}$$

The exit velocity is based on the exit pressure, exit Mach number, exit temperature, exit speed of sound, gas constant R, density of air, and specific heat ratio γ. The exit Mach number is predicated on the nozzle exit and inlet pressure and the specific heat ratio γ as shown in equation (27). The exit temperature T_{exit} depends on the exit Mach number, specific heat ratio γ, and the nozzle inlet temperature T_3 equation (28). The exit speed of sound a_{exit} is based on the exit temperature T_{exit}, gas constant R, and specific heat ratio γ equation (29). After calculating these parameters, the exit velocity V_{exit} of the nozzle is estimated by multiplying the exit Mach number with the exit speed of sound, equation (30). The exit air density of the nozzle ρ_{exit} values is predicated using the exit pressure P_{exit}, gas constant R, and exit temperature T_{exit} equation (31). Finally, Equation (32) is used to calculate the exit mass flow rate $\dot{m}_4$ for the nonchoked flow.

$$Mach_{exit} = \sqrt{\frac{2}{\gamma - 1}\left[\left(\frac{P_3}{P_4}\right)^{\left(\frac{\gamma-1}{\gamma}\right)} - 1\right]} \tag{27}$$

$$T_{exit} = T_4 = \frac{T_3}{1 + {Mach_{exit}}^2 * \left(\frac{\gamma - 1}{2}\right)} \tag{28}$$

$$a_{exit} = \sqrt{\gamma * R * T_{exit}} \tag{29}$$

$$V_{exit} = Mach_{exit} * a_{exit} \tag{30}$$

$$\rho_{exit} = \frac{P_4}{R * T_4} \tag{31}$$

$$\dot{m}_4 = Mach_{exit} * a_{exit} * \rho_{exit} * A_{exit} \tag{32}$$

3.6.5 Thrust

The required thrust needed to drive the aircraft forward is based on the mass flow rate with the velocity difference between the inlet and outlet, and the exit percent area of the nozzle and the pressure difference between the exit and ambient, equation (33).

The inlet velocity is found by taking the square root of the input Mach number from the environment block times the specific heat ratio, gas constant and the ambient temperature, equation (34).

$$V_1 = Mach_1 * \sqrt{\gamma * R * T_1} \tag{33}$$

$$Thrust = \dot{m}_4(V_{exit} - V_1) + A_{exit}(P_{exit} - P_1) \tag{34}$$

3.7 Thrust Control System

There are two different PI controllers used in the propulsion system Simulink model: Thrust controller and exit area controller. The thrust controller is a PI controller, which is used to control the input voltage of the electrical DC motor by comparing the actual thrust of the ducted fan distributed propulsion system model with the thrust demanded of the NASA N3-X aircraft. The thrust PI controller indirectly manipulates the generated thrust via power supplied to the electric motor to be equal to the demanded thrust values (i.e. converging the error between them to zero). The output of this controller is the voltage which is the input voltage to the electrical motor that used to produce the required mechanical power for the system. Then, the mechanical power drives the ducted fan through the shaft, and then it changes the actual thrust by varying the shaft speed and the mass flow rate as illustrated in Figure 9.

The variable nozzle exit area is a PI controller, which is used to control the exit area of the convergent nozzle by comparing the actual pressure ratio of the propulsion system model to the desired or design pressure ratio of the NASA N3-X aircraft design characteristics. The PI controller adjusts the actual pressure ratio to be equal to the design pressure ratio (i.e. converging the error between them to zero) throughout the flight profile except during takeoff and landing segments which require higher thrust demands. The output of this PI controller is the exit area of the convergent nozzle that is used to calculate the thrust as showed in equation (34) and change the actual pressure ratio of the ducted fan distributed propulsion system model as illustrated in Figure 10.

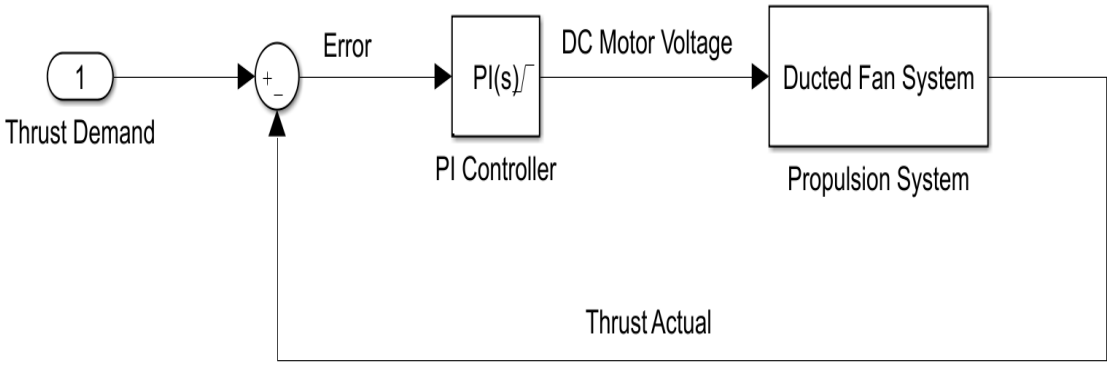

Figure 9: Electrical Motor Thrust Controller

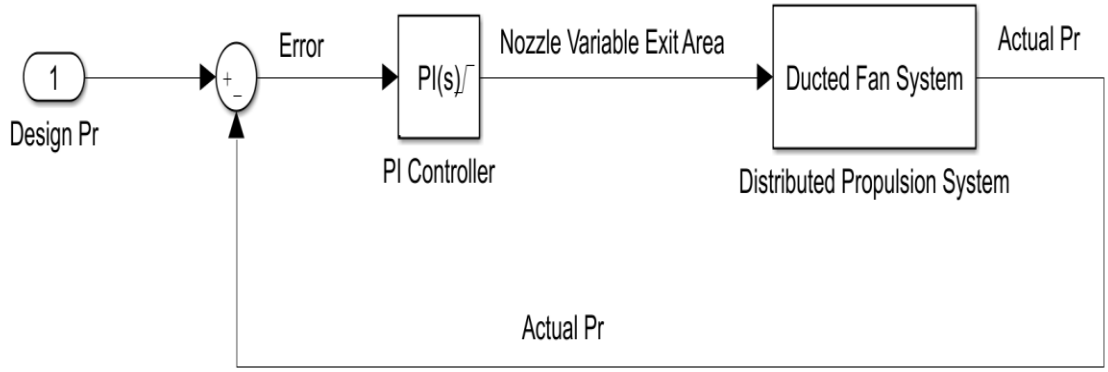

Figure 10: Nozzle Exit Area Controller

4. Results

The primary function behind modeling the distributed propulsion system of the conceptual N+3 NASA aircraft is to calculate the total aircraft thrust required, and the electrical power needed to achieve that required thrust at every time-step throughout notional flight profiles. To achieve this, NASA's next generation N+3 aircraft, N3-X, is utilized.

Three different studies with the N3-X model will be presented. The first the N3-X baseline is the Boeing 777-200LR class aircraft using NASA's defined flight. The second study uses the same aircraft with a maneuvering flight profile, In the final study, the aircraft is down sized to a 50 passenger regional transport aircraft, the Bombardier CRJ 200, flying a typical regional flight profile.

The ducted fan distributed propulsion system model is considered a model of two ducted fans, which represent the total number of the ducted fans for the three cases. For the first and second case, one of these two fans represents eight fans, and the other fan represents six back-up fans. However, for the third case; one of these fans represent two fans, and the other fan represents one back-up fan.

4.1 Fan Pressure Ratio (FPR)

An array of fan pressure ratios (FPR) were tested to investigate the influence of varying the FPR on the performance of the conceptual N3-X aircraft. The FPR is chosen based on many factors such as the ducted fan thrust, power, diameter, drag, and efficiency.

In Figure 11, there are two lines plotted, the thrust values with the FPR values and the power required for the thrust values. The FPR has chosen to be 1.3 based on Microsoft Excel sheet hand calculation. The ducted fan thrust, power, and efficiency values were calculated by using equation 5, 11, 13, 15, 16, 27, 28, 29, 30, 33, and 34 for different values of the FPR which ranged from 1.1 to 2.

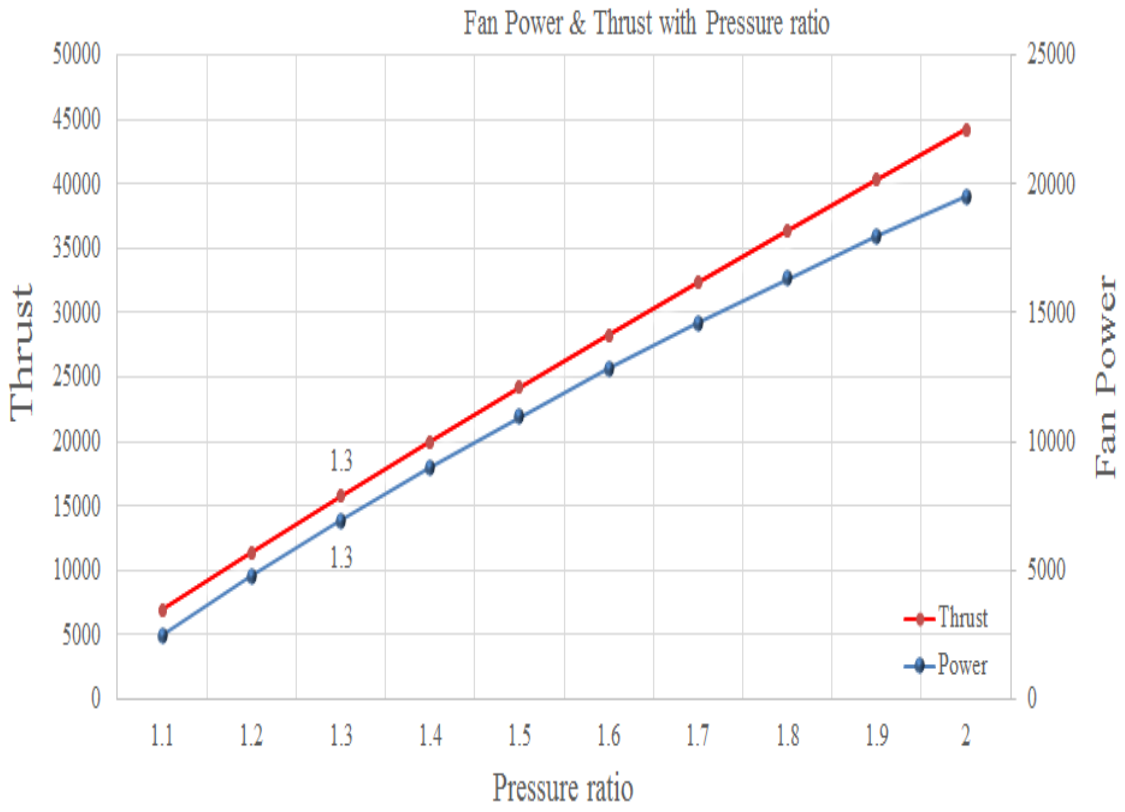

Figure 11: Ducted Fan Thrust & Power vs. Fan Pressure Ratio

It is observed that when the FPR is increased the ducted fan thrust and power required are increased therefore fixing the fan design diameter is required. This is accomplished by calculating the efficiency, which is equal to dividing the ducted fan thrust by the power for each FPR value.

The thrust to power ratio is a measure of the propulsion efficiency. Figure 12 shows the variation this efficiency with the FPR. The highest efficiency occurs when the FPR is equal to 1.3 and 2. Decreasing FPR, the effective bypass ratio values are increased while the thrust specific fuel consumption (TSFC) is decreased. From Figure 12, for FPR values lower than 1.5, the efficiency and the TSFC increase because the total pressure losses of the boundary layer ingestion (BLI) is increased. Therefore, a considerable amount of the fan total pressure is used to compensate for the total pressure losses of the BLI. As a result, more thrust is needed to produce the total pressure of the fan which leads to a decrease in the propulsive efficiency.

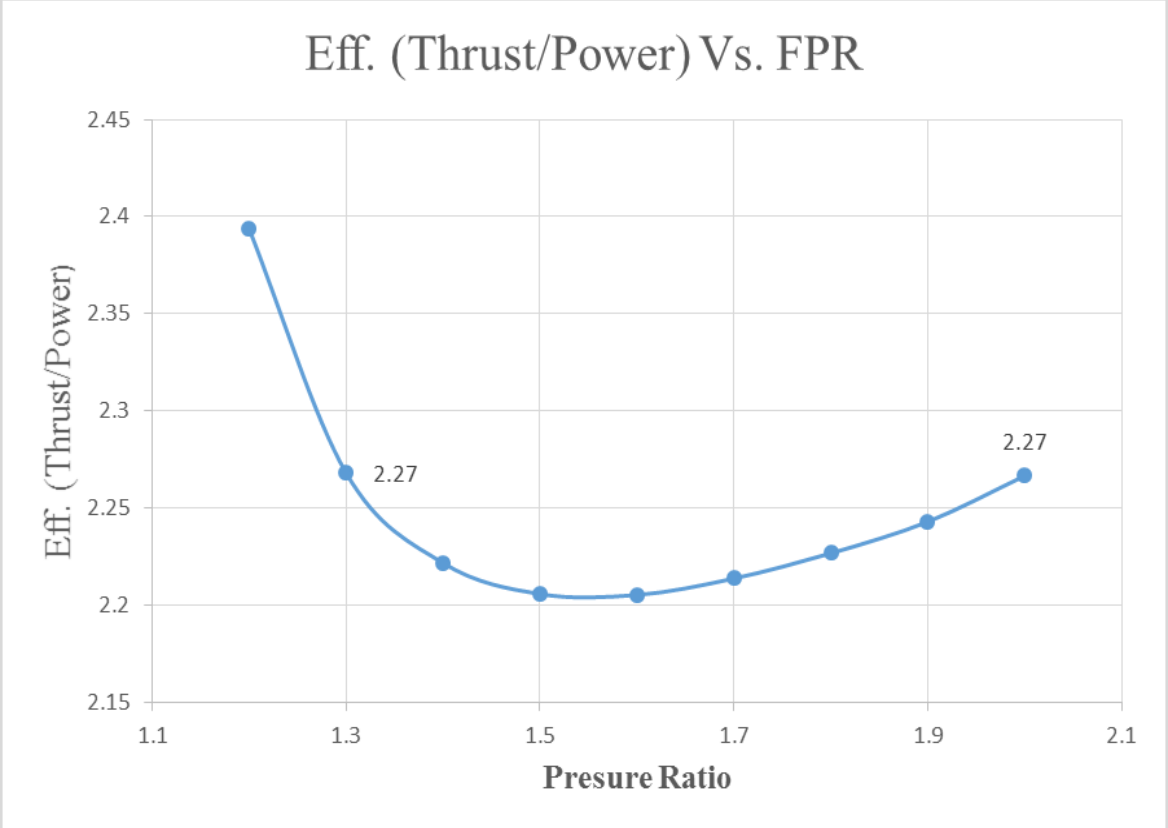

Figure 12: Efficiency vs. Fan Pressure Ratio

In order to solve the problem of the decreasing propulsive efficiency, two options are analyzed. First, increasing the power generation to compensate for the decrease in the required thrust would result in an increase in the TSFC – not a good idea! Although, increasing the fan diameter will increase the mass flow rate entering the fan, there are limits on the size of the fan. There are 14 fans and so size limitations must be considered. The drag force increases with increasing fan diameter besides the external area of the nacelle limitation. For these reasons, a FPR less than 1.2 cannot be used. A FPR of 1.3 gives the highest efficiency at a FPR which will not limit the aircraft design in other ways. An important note, this fan pressure ratio is used for all three studies.

Figure 13 is associated with Figure 12 based on NASA Glenn Research Center which shows, the variation of the TSFC with the FPR. The lowest TSFC occurs when the FPR is equal to 1.3.

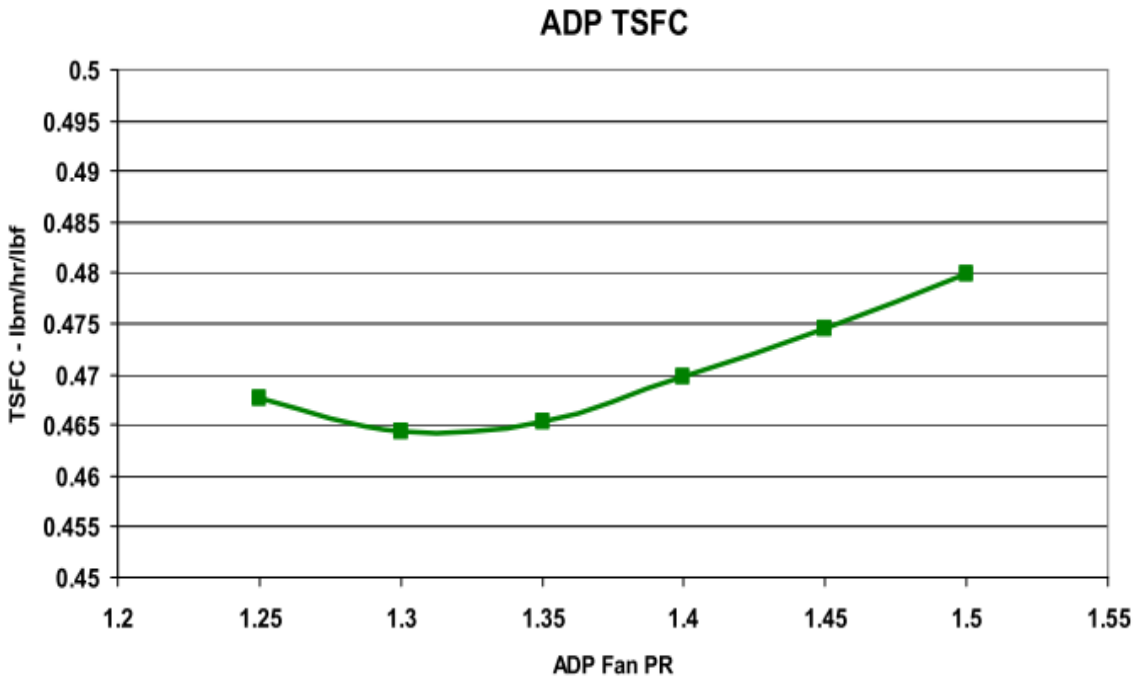

Figure 13: TSFC vs. Fan Pressure Ratio[11]

4.2 Boeing 777-200LR with an Actual Flight Profile

4.2.1 Baseline Flight Profile

The ducted fan distributed propulsion system model is used to simulate an actual flight profile of NASA's N3-X (Boeing 777-200 LR class airplane). The Boeing 777-200 LR airplane travels from Istanbul Ataturk Airport to John F. Kennedy International Airport, Figure 14. The Mach number and altitude vary throughout the flight profile. The altitude starts from 0 ft and climbs to the maximum altitude at 37 Kft. After the cruise segment of the flight, it returns to 0 ft at the end of the flight profile. The Mach number starts from 0.1 reaching the maximum Mach number of 0.85 before returning to 0.35 at the end of the flight profile.

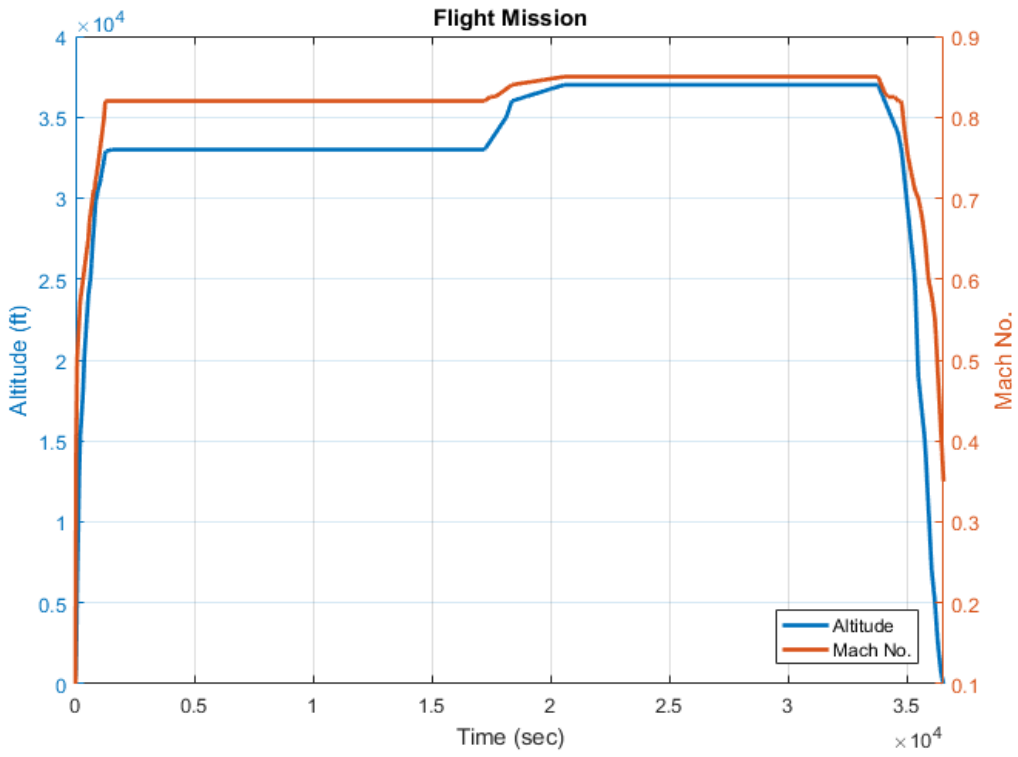

Figure 14: Baseline Flight Profile

4.2.2 Thrust Actual and Thrust Demand

The thrust is considered the main output of the ducted fan distributed propulsion system model. There are two types of thrust: generated and demand thrust. Thrust generated is the thrust produced by the ducted fan distributed propulsion system, while the thrust demanded is the required thrust needed for the N3-X aircraft. As a result, the thrust generated should match the thrust demanded throughout the flight profile. The thrust demanded values of the flight were chosen according to the NASA/Cranfield University analysis. Figure 15 below shows the thrust generated and demanded throughout the flight for one fully operational fan. In Figure 16, one of the six back-up fan's thrust is shown.

In Figure 15, the thrust actual is identical to the thrust demanded across the flight profile. Notice, the maximum thrust occurs through the takeoff and climb leg until the aircraft reaches the maximum altitude and starts the cruise segment. At the end of the cruise segment, the thrust values decrease until the descent segment. After that, the thrust values increase in the transition area until the values reach the approach and landing segment. When the approach segment ends, the thrust values decrease throughout the landing and taxi segments until the aircraft has stopped at 0 thrust.

In Figure 16, the thrust generated versus thrust demanded for the back-up fans is shown. Again, the agreement between the two thrust levels is excellent. The thrust profile clearly shows that the back-up fans are not used except for the high thrust demand segments of the flight. This performance is by design.

The thrust values start at 0 KN and increase on the runway until reaching the maximum thrust value at takeoff. Then the thrust begins to decrease in the transition until the thrust reaches 0 KN. After the cruise and descent segments end, the thrust values began to

increase until they reached the approach and landing thrust. When the approach ends, the thrust decreases throughout the landing and taxi segments until the aircraft stops at 0 KN.

Figure 17 shows, the total thrust generated and thrust demanded throughout the flight. Similar to Figures 15 and 16, the agreement between the thrust generated and demanded is excellent throughout the flight.

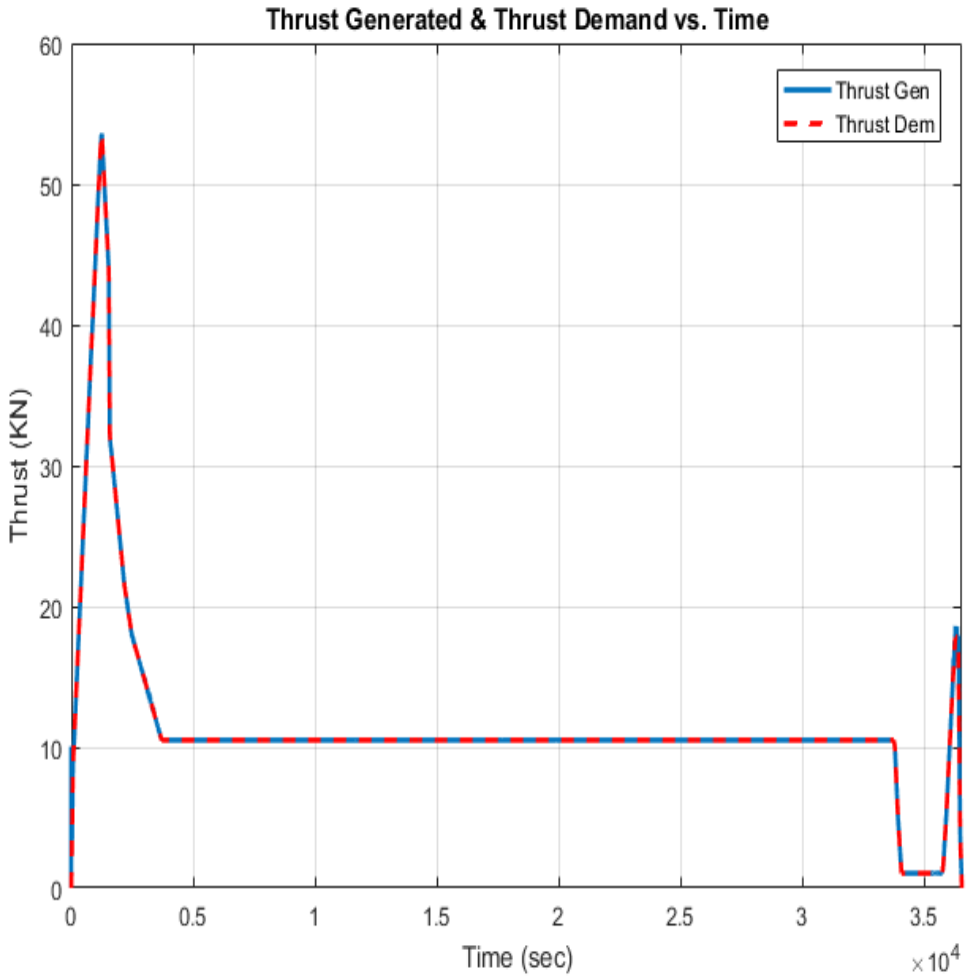

Figure 15: Thrust Generated and Demand For One Continuous Operation Fan

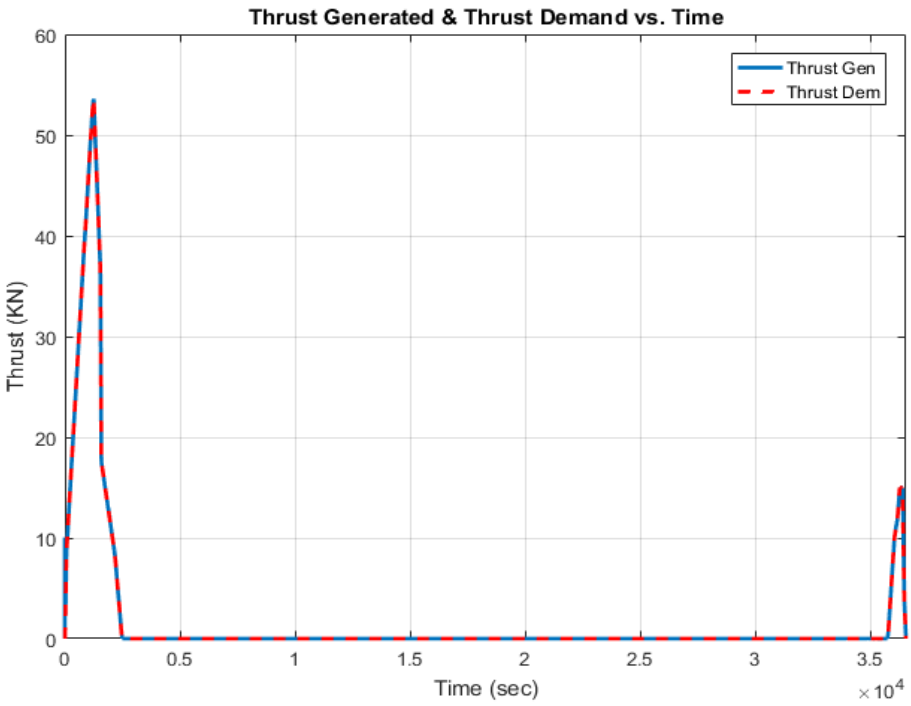

Figure 16: Thrust Generated and Demand For One Fan of Six Back-up Fans

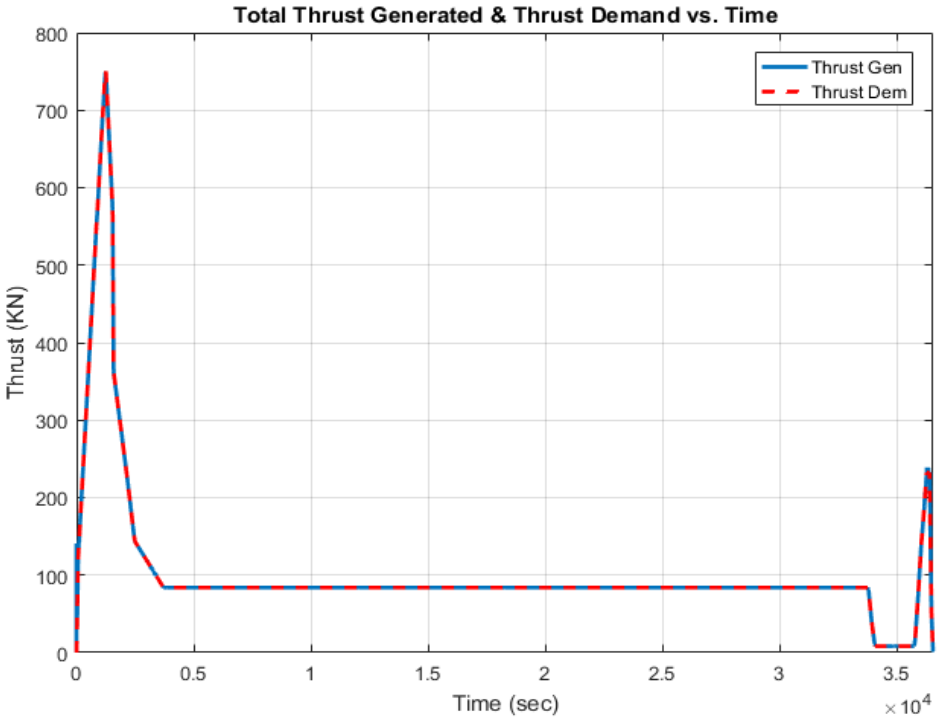

Figure 17: The Total Thrust Generated and Demand For Fourteen Fans

4.2.3 Power Required

The power is considered the primary input of the ducted fan distributed propulsion system model. There are three types of power: electrical power, net or mechanical power, and total power losses. First, electrical power is the total power used to drive the electrical DC motor of the ducted fan distributed propulsion system. The mechanical power is the net power used to drive the fan's shaft. The electrical power losses include the electrical DC motor losses (i.e. hysteresis, eddy current, armature, and windage). This loss is important to estimate for future thermal management studies of the electrical propulsion system. The electrical power is calculated in the ducted fan distributed propulsion system model depending on the required thrust of the N3-X aircraft. Using the control system the required voltage needed to produce the required thrust is determined.

Figure 18 shows the electrical power, net or mechanical power, and total electrical power losses throughout the flight for one of the continuous operating fans. Figure 19 shows the electrical power, net or mechanical power, and total power losses throughout the flight for one of the back-up operation fans.

The electrical power starts at 0 MW when the aircraft on the ground, and the electrical power starts to increase on the runway until reaching maximum electrical power at takeoff. After that, the electrical power begins to decrease until it arrives at the cruise segment power. After the cruise segment ends, the electrical power decreases until reaching the descent segment electrical power. Next, the electrical power begins to increase until reaching the approach and landing power. When the approach ends, the electrical power begins to decrease throughout the landing and taxi segment until the aircraft is ready to shut down or stop, and at that moment the electrical power is 0 MW.

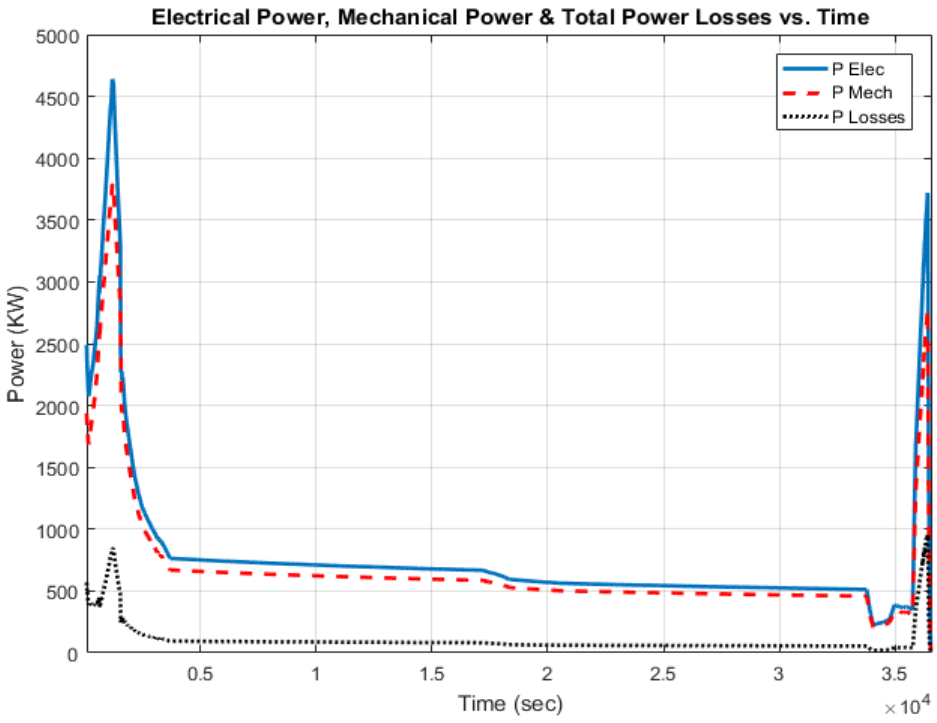

Figure 18: The Electrical, Mech. & Losses Power for One Continuous Operation Fan

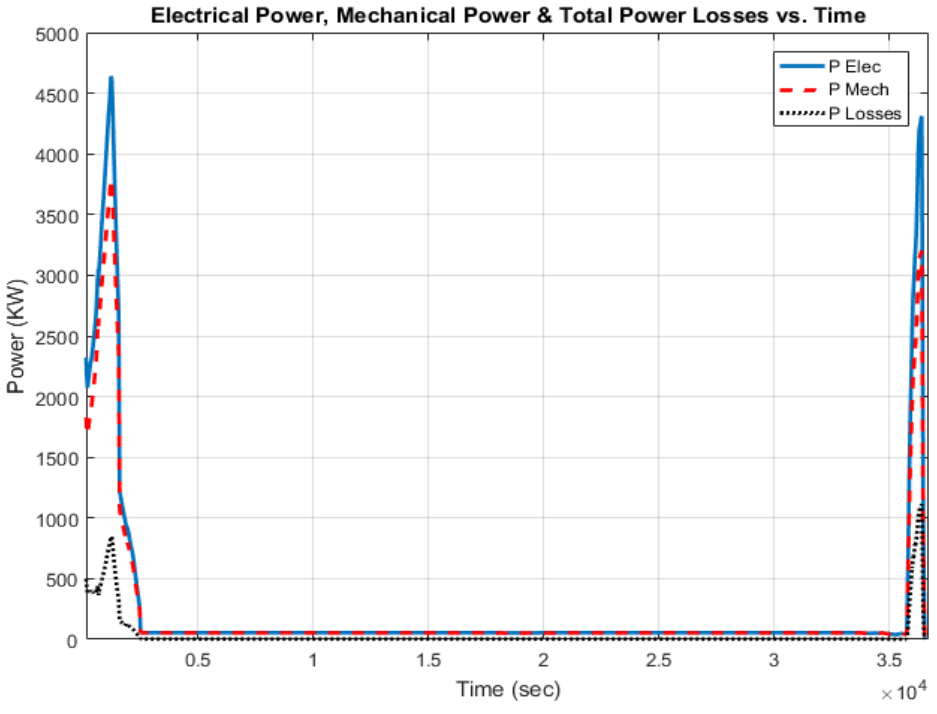

Figure 19: The Electrical, Mechanical & Losses Power For One Fan of Six Back-up Fans

Figure 19 shows, the electrical power for the back-up operation fans over the flight. The electrical power starts at 0 MW when the aircraft on the ground. The electrical power starts to increase on the runway until reaching the maximum electrical power at the takeoff segment. Next, the electrical power begins to decrease until reaching a zero level throughout the cruise and descent segment. After the cruise and descent segment ends, the electrical power begins to increase until reaching the approach and landing segment electrical power. When the approach segment ends, the electrical power begins to decrease throughout the landing and taxi segments until the aircraft has stopped, when at that moment the electrical power is equal to 0 MW.

Figure 20 shows the total electrical, mechanical, and losses power throughout the flight for all of the ducted fans. The total electrical power starts at 0 MW and increases on the runway until reaching the maximum electrical power of 64.6 MW at takeoff. Then, the total electrical power begins to decrease until reaching the cruise segment power which is 10.2 MW. After the cruise segment ends, the total electrical power decreases until the descent segment electrical power of 2.1 MW is reached. Next, the total electrical power begins to increase until reaching the approach and landing segments when electrical power which is 54 MW. When the approach ends, the electrical power begins to decrease throughout the landing and taxi-in segment until the aircraft stops, where the electrical power is 0 MW.

The electrical power results throughout the flight profile were compared with NASA and Cranfield University [15][17] studies.

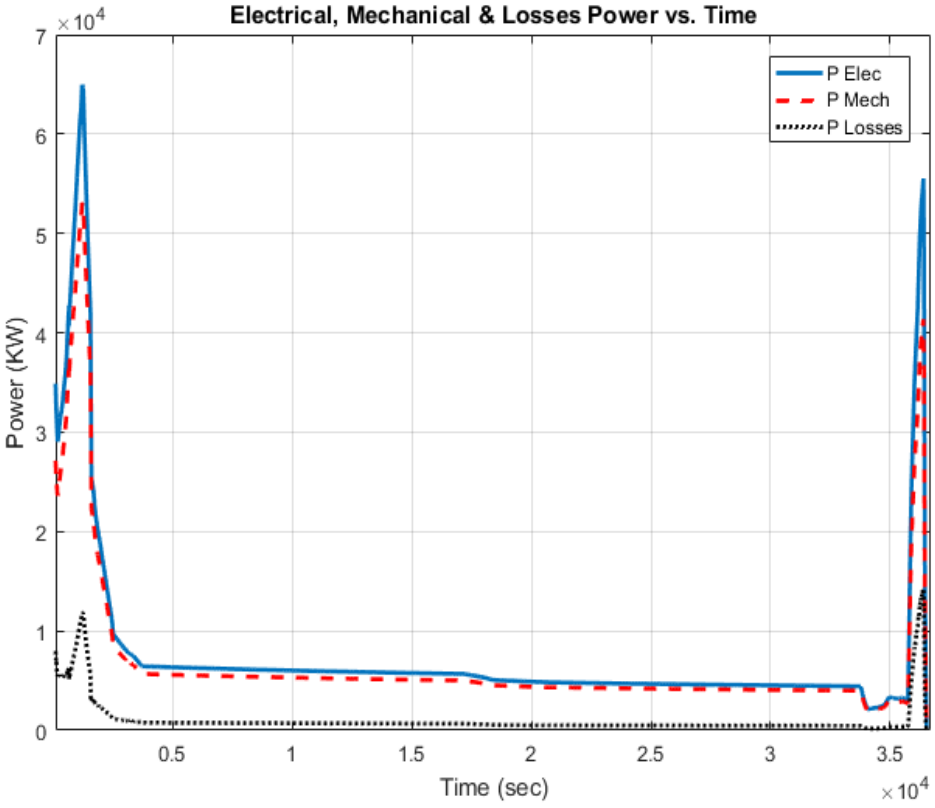

Figure 20: The Total Elec, Mech., Loss Power for Fourteen Fans

4.2.4 Electrical Motor

4.2.4.1 Electrical Motor Voltage

The input voltage of the electrical DC motor is the source of the electrical power. The thrust control system determines the input voltage values by matching the thrust generated and the thrust demanded throughout the flight, varying the input voltage which is the output of this controller. The voltage is input to the electrical DC motor to produce the electrical power of the ducted fan distributed propulsion system model.

Figure 21 shows the input voltage over the flight for one fan of the continuous operating fans. The back-up fans input voltage is shown in Figure 22.

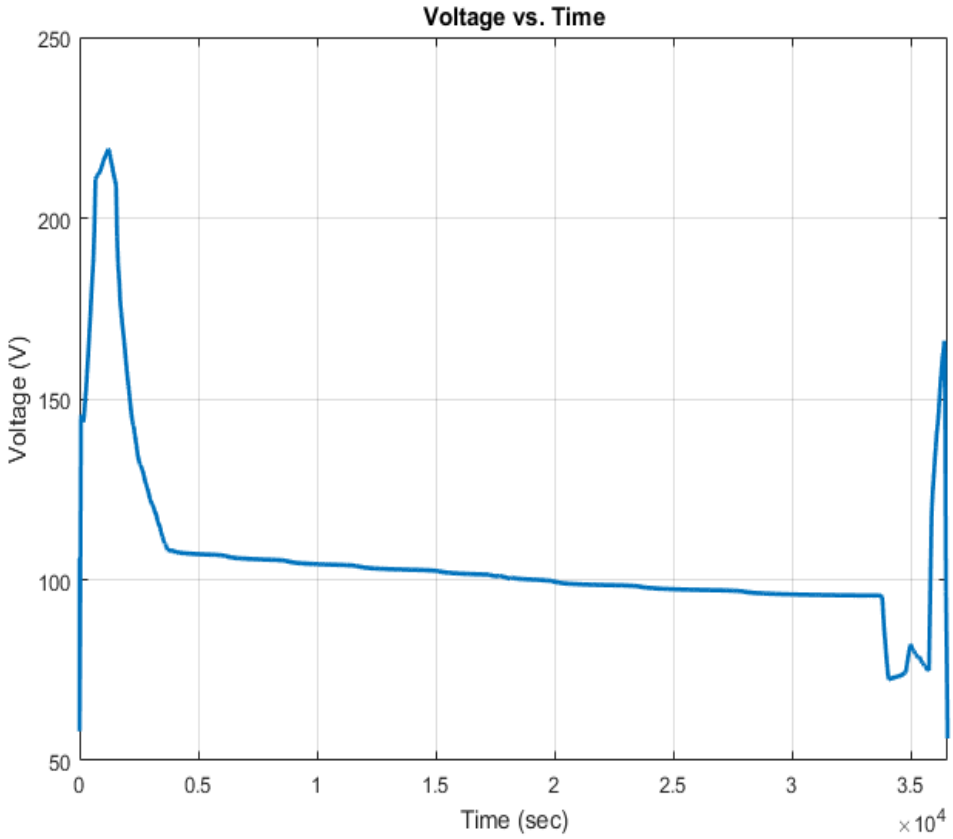

Figure 21: The Input Voltage of The DC Motor for One Continuous Operation Fan

The maximum input voltage is for the takeoff and climb segment until the aircraft reaches the highest point. Also, a high voltage (electrical power) is required for the approach and landing segment. The input voltage starts from 100 V, which is the initial value. As the model proceeds, the PI controller determines the input voltage based on the thrust generated and demanded. For instance, the maximum voltage, which is equal to 219 V, is at the end of the takeoff segment and the highest climb point where the Mach number is 0.82 and the altitude is 32.9 Kft. The voltage values decrease to 133 V for cruise and the voltage continued to decrease to 74 V during descent. After descent, the voltage is increased to 166 V for the approach and landing segment. When the approach segment is ending, the voltage values began to decrease throughout the landing and taxi segment

until the aircraft stopped at 0 V.

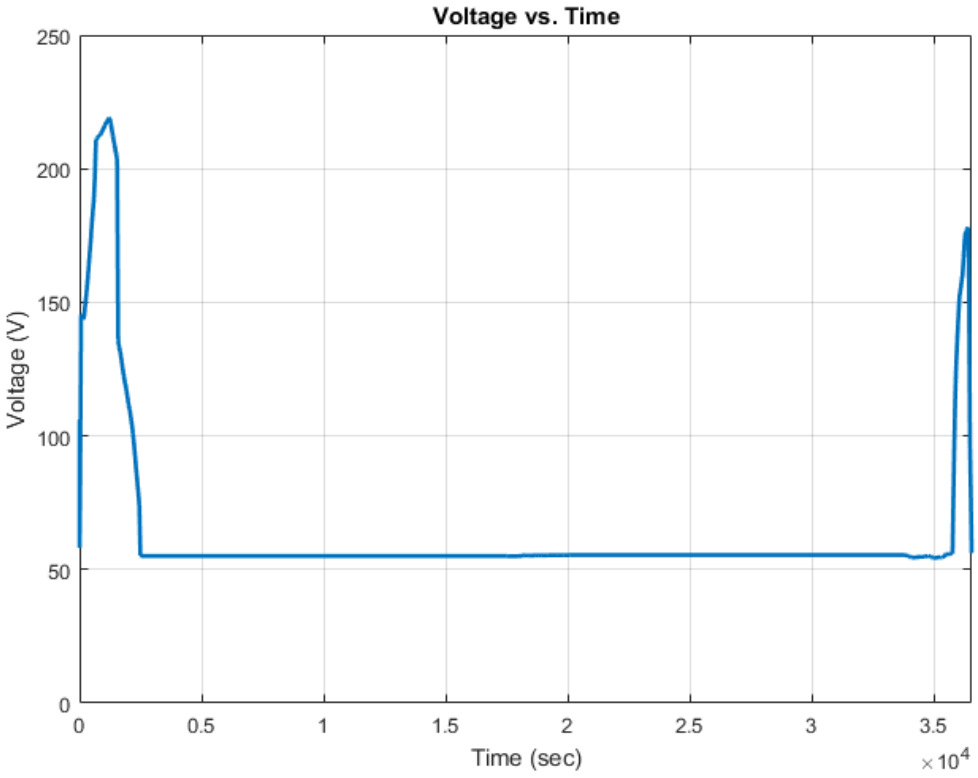

Figure 22: The Input Voltage of The DC Motor for One Fan of Six back-up Fans

The input voltage plots in Figure 21 and Figure 22 are similar in behavior. The maximum input voltage is for the takeoff and climb segment until the aircraft reaches the highest point of climbing. Also, voltage (electrical power) is required for the approach and landing segment.

The input voltage starts from 100 V, which is the initial value. Next, the PI controller determines the input voltage based on the thrust generated and demanded. For instance, the maximum voltage, which is equal to 219 V, is at the end of the takeoff and the highest climb point where the Mach number is 0.82, and the altitude is 32.9 Kft. The input voltage values decrease to 58 V for the cruise and descent segment. After the cruise and

descent segment end, the input voltage begins to increase to 176 V for the approach and landing segment. When the approach segment is ending, the input voltage values began to decrease throughout the landing and taxi segment until the aircraft stopped at 0 V.

4.2.4.2 Electrical Motor Efficiency

The efficiency of the electrical DC motor is very high, and depends on the net or mechanical power, as well as the total or electrical power. Equation (5) in the methodology is used to calculate the efficiency values.

The graphical representation of the electrical motor efficiency is shown in Figure 23 below; Figure 23 shows the efficiency throughout the flight for one fully operational fan. Figure 24 shows the graphical representation of the electrical motor efficiency throughout the flight for one of the six back-up fans.

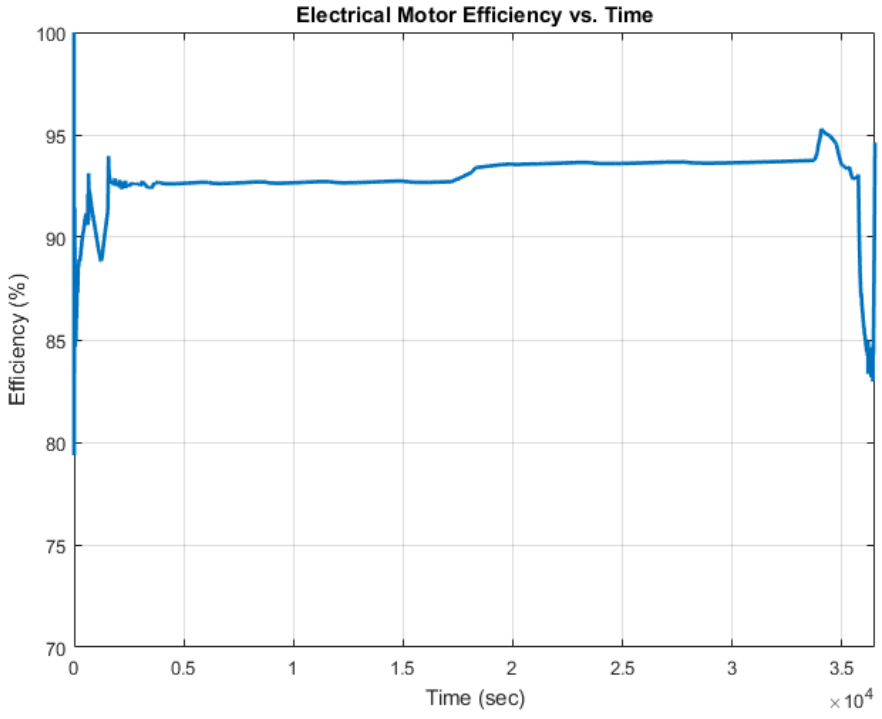

Figure 23: The DC Motor Efficiency for One Continuous Operation Fan

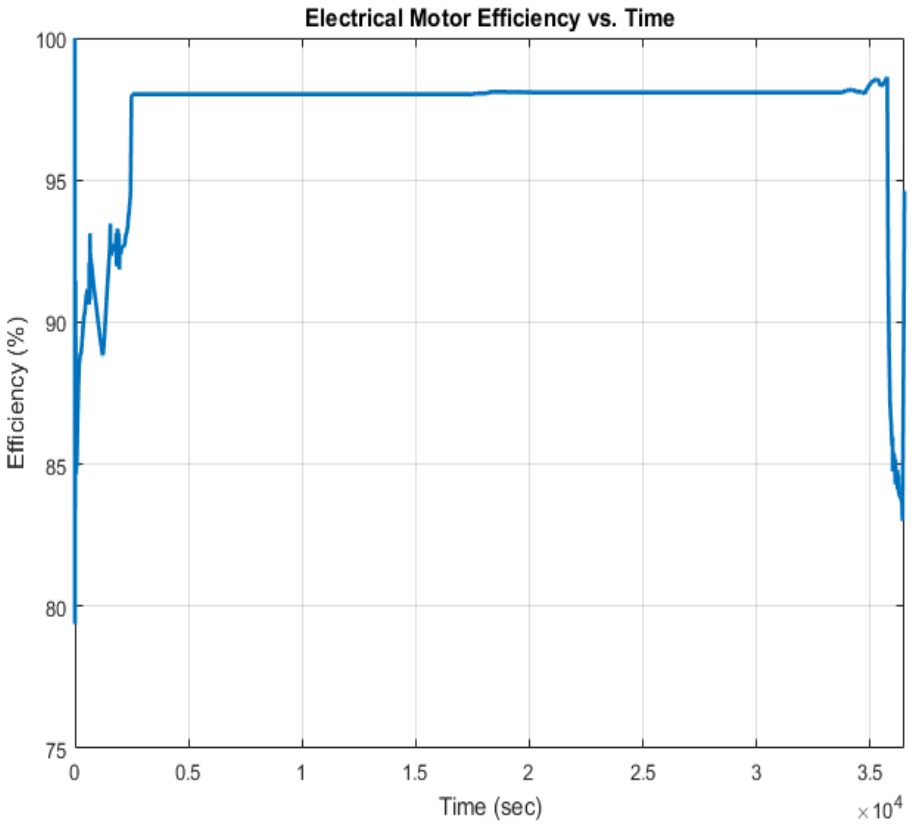

Figure 24: The DC Motor Efficiency for One Fan of Six Back-up Fans

4.2.5 Pressure

The pressure parameter is considered one of the critical parameters that need to make up the boundary conditions of the ducted fan distributed propulsion system model. The inlet pressure to the ducted fan and the outlet pressure of the fan (or the inlet pressure to nozzle) are deemed the important pressures states in the propulsion system because they determine the fan pressure ratio that affects the performance of the conceptual N3-X aircraft. The environment subsystem block provides the inlet pressure to the fan, while the mixer or plenum volume calculates the outlet pressure of the fan.

The graphical representations of the pressures are shown in Figure 25 below. The input

and output pressure of the ducted fan throughout the flight for one fully operational fan is presented. Figure 26 presents input and output pressure of the ducted fan throughout the flight for one of the six back-up fans.

The initial value of the outlet pressure had been chosen to be equal to 106 KPa which is equal to the inlet total pressure at the ground. The outlet pressure starts at 106 KPa which is the initial value at the beginning, then the outlet pressure values increase until reaching the takeoff segment pressure, which is 160 KPa. After that, the pressure values decreases to 134 KPa where the Mach number is 0.82 and the altitude is 32.9 Kft, which is considered the highest point. Then, the outlet pressure decreases in the transition to reach 70-64 KPa at the cruise segment, and the values continue to decrease reaching 44 KPa at the descent. After the descent segment, the outlet pressure values increase in the transition area to be 188 KPa at the approach and landing segment. Then, the outlet pressure begins to decrease throughout the landing and taxi segment until the aircraft is ready to shut down or stop. At that moment, the outlet pressure of the fan is 110 KPa which is equal to the inlet total pressure of the fan.

However, the inlet pressure starts at 105 KPa which is the ambient total pressure, and the values increase to reach the maximum value which is 111 KPa at the takeoff segment on the runway. Then, the inlet pressure values decrease until the values reach 49-41 KPa at the cruise flight, and they continued to decrease to reach 34 KPa at the descent. After the descent segment, the inlet pressure values increase in the transition, approach, and landing segment until the aircraft is ready to shut down or stop. At that moment, the inlet pressure value is equal to the outlet pressure of the fan, and they are 110 KPa.

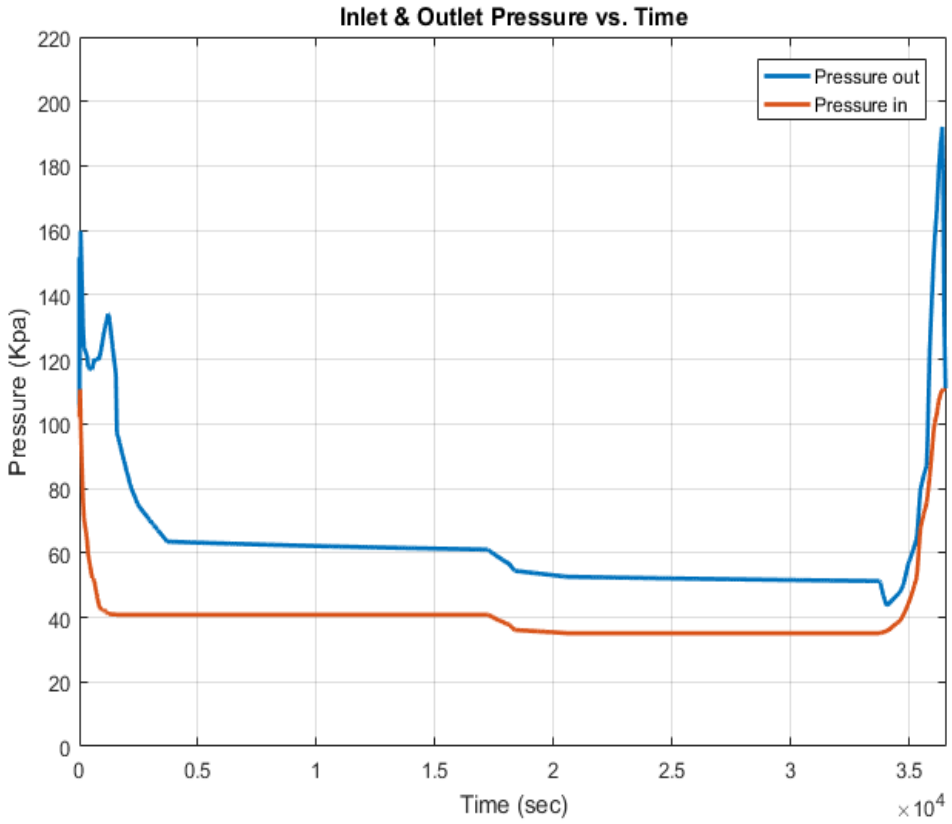

Figure 25: The Inlet and Outlet Pressure for One Continuous Operation Fan

It is significant to notice that the pressure and especially the inlet pressure of the ducted fan values are dependent on the altitude values. Moreover, the pressure has an inverse relationship with the altitude. For instance, when the cruise segment is starting, the pressures are going be to decrease to the minimum because of the highest altitude in the cruise segment.

The inlet and outlet pressure of the ducted fan plots in Figure 25 and Figure 26 have some similarities in behavior throughout the takeoff and landing segment. The initial value of the outlet pressure had been chosen to be equal to 106 KPa which is equal to the inlet total pressure at the ground. The outlet pressure starts at 106 KPa which is the initial value at the beginning, then the outlet pressure values increase to reach 160 KPa at the

takeoff segment on the runway. Then, the pressure decreases to reach 134 KPa where the Mach number is 0.82 and the altitude is 32.9 Kft, which is considered the highest point. After that, the outlet pressure begins to decrease in the transition area until it is near to the inlet pressure which is 43 KPa, where the back-up fan starts to decrease its speed to the minimum speed (i.e., it stops producing considerable thrust) throughout the cruise and descent segment. After the cruise and descent segment end, the outlet pressure begins to increase in the transition area to be 200 KPa at the approach and landing segment. When the approach segment ends, the values decrease throughout the landing and taxi segment until the aircraft is ready to shut down or stop. At that moment, the outlet pressure of the fan value is equal to 110 KPa which is equal to the inlet total pressure of the fan.

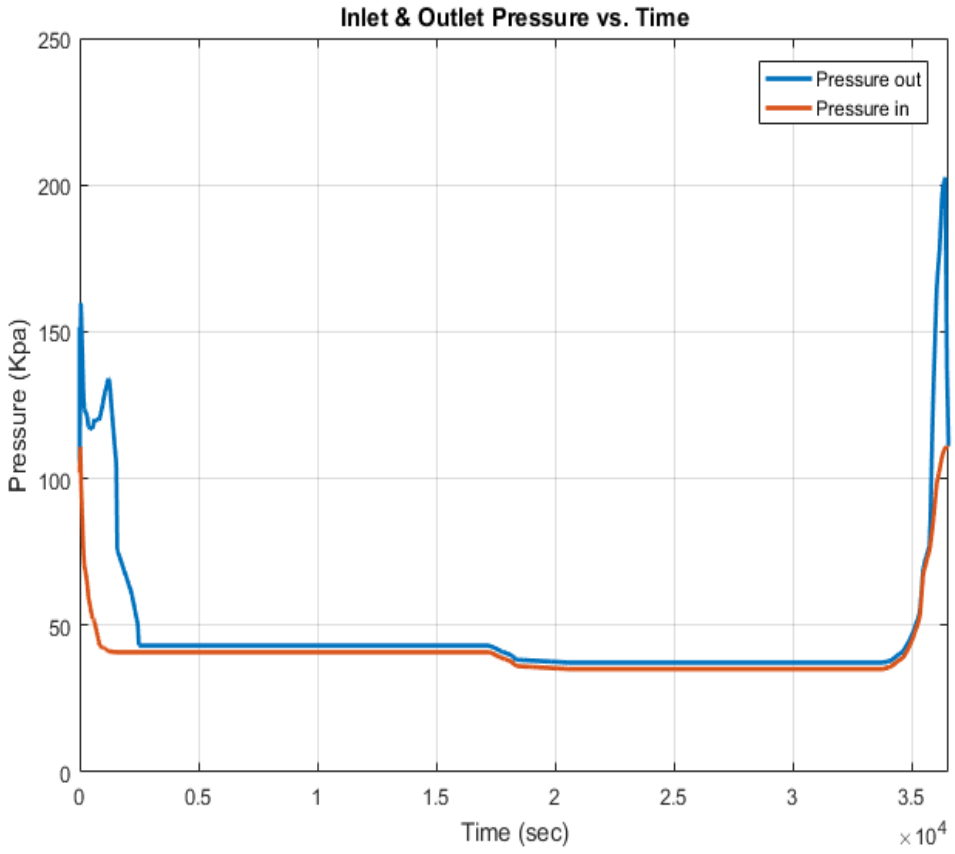

Figure 26: The Inlet and Outlet Pressure for One Fan of Six Back-up Fans

However, the inlet pressure of the ducted fan plot is the same inlet pressure in Figure 25. Also, the inlet pressure starts at 105 KPa which is the ambient total pressure, and the values increase to reach the maximum value which is 111 KPa at the takeoff segment on the runway. Then, the inlet pressure values decrease until they reach 41 KPa at the cruise segment, and the values continue to decrease to reach 34 KPa at the descent. After the descent segment ends, the inlet pressure values increase in the transition, approach, and landing segment until the aircraft is ready to shut down or stop. At that moment, the inlet pressure value is equal to the outlet pressure of the fan, and they are 110 KPa.

4.2.6 Temperature

The temperature parameter is deemed one of the essential parameters that are needed to make up the boundary conditions of the ducted fan distributed propulsion system model. Also, the inlet temperature to the ducted fan and the outlet temperature of the fan (or the inlet temperature to nozzle) are considered the important types of the temperatures in the propulsion system because they are used to calculate the fan work or fan power needed to operate the fan and other benefits. The environment subsystem block provides the inlet temperature to the fan, while the outlet temperature is calculated by using Equation 13 inside the fan subsystem block.

The temperature and specifically the inlet temperature of the ducted fan values are dependent on the pressure of the ducted fan, as well as the altitude values. In addition, the temperature parameter has a proportional relationship with the pressure parameter and an inverse relationship with the altitude. For example, the inlet and the outlet temperature of the ducted fan plots in Figure 27 and 28 are similar to the inlet and outlet pressure of the

ducted fan plots in Figure 25 and 26 by following the same behavior.

The graphical representations of the temperature types in Figure 27 below, shows the input and output temperature of the ducted fan throughout the flight for one fully operational fan. Figure 28 shows the graphical representations of the temperature types which are the input and output temperature of the ducted fan throughout the flight for one of the six back-up fans.

The outlet temperature is dependent on the inlet and outlet pressure, inlet temperature, isentropic efficiency, and specific heat ratio.

The outlet temperature starts at 291 K which is the first calculated value of the outlet temperature at the beginning. Then the outlet temperature values increase to reach 323 K at the takeoff on the runway. After that, the temperature values decreases to 321 K where the Mach number is 0.82 and the altitude is 32.9 Kft, which is considered the highest point. Then, the outlet temperature values decrease in the transition area to reach 265 K at the cruise segment, and the values continue to decrease to reach 232 K at the descent. After the descent ends, the outlet temperature values increase in the transition area to be 336 K at the approach and landing segment. When the approach segment ends, the values decrease throughout the landing and taxi segment until the aircraft is ready to shut down or stop. At that moment, the outlet temperature of the fan value is 289 K which is almost equal to the inlet total temperature of the fan.

However, the inlet temperature starts at 288 K which is the ambient total temperature. Then, the inlet temperature values decrease until the inlet temperature values reach 222 K at the cruise segment, and the values continue to decrease to reach 218 K at the descent segment. After the descent segment, the inlet temperature values are increased in the

transition area, approach, and landing segment until the aircraft is ready to shut down or stop. At that moment, the inlet temperature value is equal to the outlet temperature value of the fan, and they are 288 K.

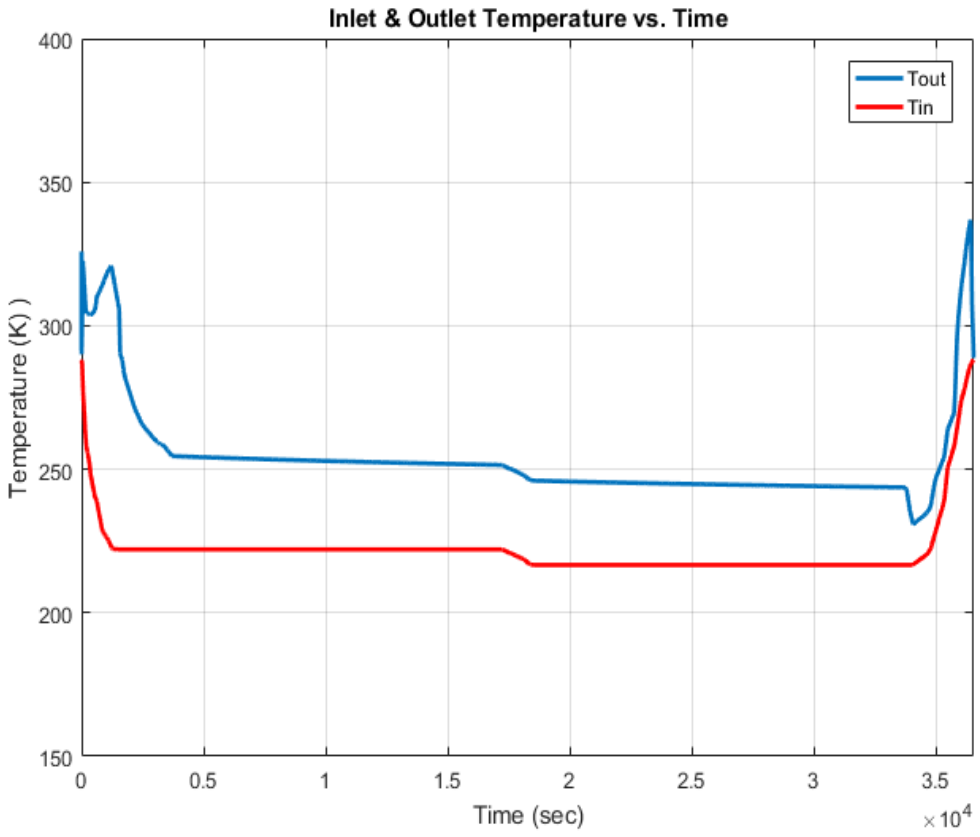

Figure 27: The Inlet and Outlet Temperature for One Continuous Operation Fan

In Figure 28 and Figure 27, the inlet and outlet temperature of the ducted fan plots are kind of similar in behavior. The maximum outlet temperature of the fan is achieved during the takeoff on the runway, approach, and landing segment.

The outlet temperature starts at 291 K which is the first calculated value of the outlet temperature at the beginning, then the outlet temperature values are increased to reach 323 K at the takeoff on the runway. After that, the temperature values decrease to reach

321 K where the Mach number is 0.82 and the Altitude is 32.9 Kft, which is considered the highest point. The outlet temperature values decrease in the transition area until it is almost the same as the inlet temperature values which are 226 K, where the back-up fan starts to decrease its speed to the minimum speed (i.e., it stops producing considerable thrust) throughout the cruise and descent segment. After the cruise and descent segment ends, the outlet temperature values increase in the transition area to be 340 K at the approach and landing segment. When the approach segment ends, the values decrease throughout the landing and taxi segment until the aircraft is ready to shut down or stop. At that moment, the outlet temperature of the fan value is 288 K which is equal to the inlet temperature of the fan.

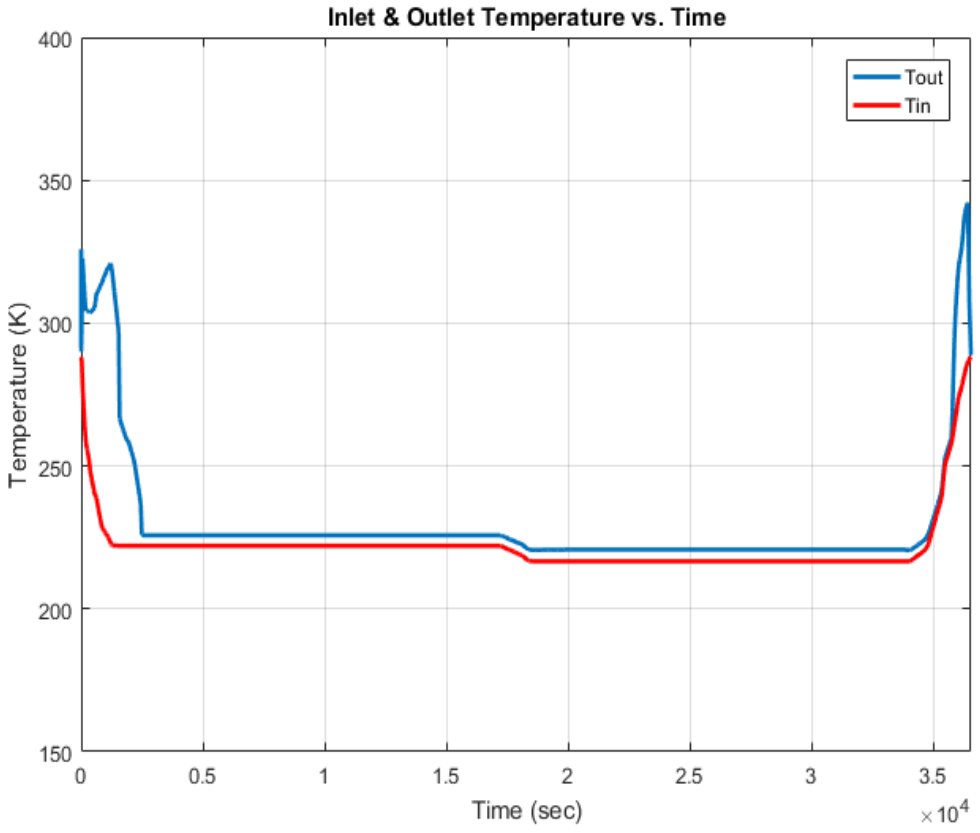

Figure 28: The Inlet and Outlet Temperature for One Fan of Six Back-up Fans

However, the inlet temperature of the ducted fan plot in this figure is the same inlet temperature in Figure 27. Also, the inlet temperature starts at 288 K which is the ambient total temperature. Then, the inlet temperature values are decreased until the inlet temperature values reach 222 K at the cruise, and the values continued to decrease to reach 218 K at the descent segment. After the descent segment, the inlet temperature values increase in the transition area, approach, and landing segment until the aircraft is ready to shut down or stop. At that moment, the inlet temperature value is equal to the outlet temperature value of the fan, and they are 288 K.

4.2.7 Velocity

One of the critical parameters needed to make up the boundary conditions of the ducted fan distributed propulsion system model is the air velocity. Also, the inlet velocity to the ducted fan and the exit velocity are such essential parameters because they are used to calculate the thrust of the ducted fan propulsion system. The environment subsystem block provides the Mach number, specific heat ratio, gas constant, and ambient temperature to calculate the inlet velocity by using Equation 33. However, the exit velocity is calculated inside the nozzle subsystem block by using Equation 25 and 30 that depend on the inlet and outlet pressure and temperature of the nozzle, gas constant, and specific heat ratio.

The velocity and especially the inlet velocity parameter are dependent on the Mach number and the speed of sound (i.e., Temperature), where the relationship between the velocity, Mach number, and speed of sound are a proportional relationship. For instance, when the Mach number is increased, the inlet velocity is increased too, Figure 29.

The diagrammatic representations of the velocity types are shown in Figure 29 below that shows the inlet and exit velocity of the propulsion system throughout the flight for one fully operational fan. Figure 30 shows the diagrammatic representations of the velocity types are the inlet and exit velocity of the ducted fan propulsion system throughout the flight for one of the six back-up fans.

Figure 29 shows that the inlet and exit velocity of the ducted fan propulsion system. The maximum exit velocity of the nozzle needs along the takeoff on the runway, approach and landing segment, and a high exit velocity of the nozzle needs throughout the climb segment.

The exit velocity of the nozzle starts at 111 m/s which is the first calculated value of the exit velocity at the beginning. Then the exit velocity values are increased to reach 329 m/s at the takeoff on the runway. After that, the velocity values decrease and then increase to reach 327 m/s where the Mach number is 0.82 and the altitude is 32.9 Kft, which is considered the highest climb point. Then, the exit velocity values decrease in the transition area to reach 299 m/s at the cruise segment, and the values continue to decrease to reach 280 m/s at the descent segment. After the descent segment, the exit velocity values increase in the transition area to be 336 m/s at the approach and landing segment. When the approach segment ends, the values begin to decrease throughout the landing and taxi segment until the aircraft is ready to shut down or stop. At that moment, the exit velocity of the nozzle value is 122 m/s which is almost equal to the inlet velocity of the nozzle value.

However, the inlet velocity starts at 34 m/s and depends on the Mach number and speed of sound on the ground. Then, the inlet velocity values are increased until they reach 245

m/s at the cruise segment. The values continued to increase to reach the highest inlet velocity value which is equal to 251 m/s where the Mach number is 0.85 and the altitude is 37 Kft, which is considered the highest cruise segment points. After that, the inlet velocity begins to decrease to reach 244 m/s at the descent segment. After the decent segment, the inlet velocity values continue to decrease in the transition area, approach, and landing segment until the aircraft is ready to shut down or stop. At that moment, the inlet velocity value is almost equal to the exit velocity of the nozzle value, and they are 119 m/s.

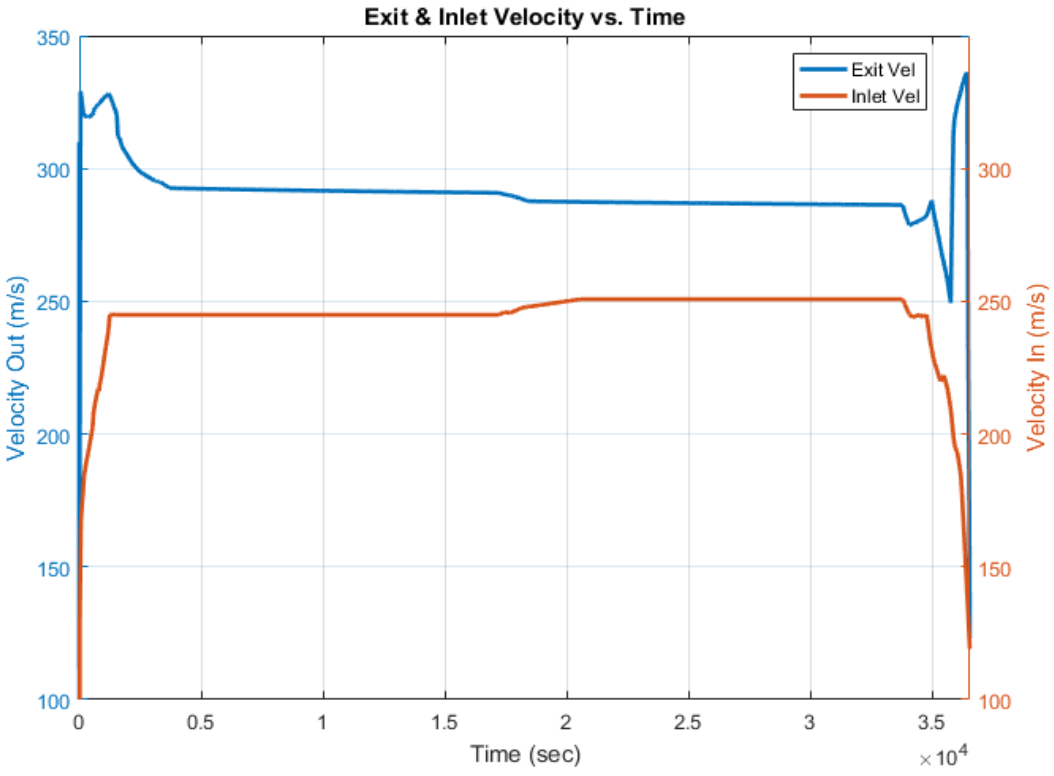

Figure 29: The Inlet and Exit Velocity for One Continuous Operation Fan

Figure 30 illustrates that the inlet and exit velocity of the propulsion system plots behavior is kind of similar to the inlet and exit velocity of the ducted fan propulsion system plots in Figure 29. The maximum exit velocity of the nozzle is only needed along

the takeoff on the runway, approach, and landing segment. Also, a high exit velocity of the nozzle is needed throughout the climb segment.

The exit velocity of the nozzle starts at 111 m/s which is the first calculated value of the exit velocity at the beginning, then the exit velocity increases to reach 329 m/s at the takeoff on the runway. After that, the velocity decreases and then increases to reach 328 m/s where the Mach number is 0.82 and the altitude is 32.9 Kft which is considered the highest climb point. Then, the exit velocity values are decreased in the transition area until they reached to values precisely equal to the inlet velocity values which are 245-251 m/s throughout the cruise and descent segment. After the cruise and descent segment end, the exit velocity begins to increase in the transition area to be 337 m/s at the approach and landing segment. When the approach segment ends, the values begin to decrease throughout the landing and taxi until the aircraft is ready to shut down or stop. At that moment, the exit velocity of the nozzle value is 122 m/s which is almost equal to the inlet velocity of the nozzle value.

However, the inlet velocity of the ducted fan propulsion system plot in this figure is the same inlet velocity in Figure 29. Also, the inlet velocity starts at 34 m/s and depends on the Mach number and the speed of sound on the ground. Then, the inlet velocity values are increased until the inlet velocity values reach 245 m/s at the cruise segment. The values continued to increase to reach the highest inlet velocity value which is equal to 251 m/s where the Mach number is 0.85 and the altitude is 37 Kft, which is considered the highest cruise points. After that, the inlet velocity values begin to decrease to reach 244 m/s at the descent. After the decent segment, the inlet velocity values continue to decrease in the transition area, approach, and landing until the aircraft is ready to shut

down or stop. At that moment, the inlet velocity value is almost equal to the exit velocity of the nozzle value, and they are 119 m/s.

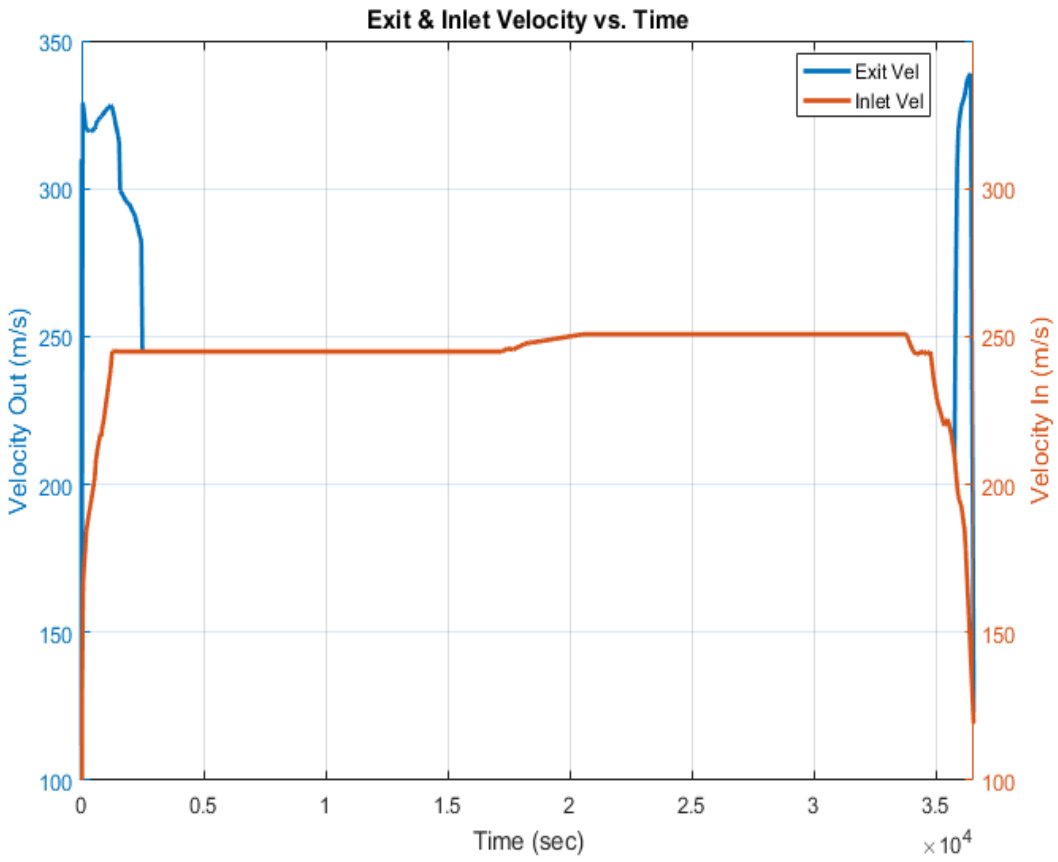

Figure 30: The Inlet and Exit Velocity for One Fan of Six Back-up Fans

4.2.8 Nozzle Exit Area

The nozzle exit area has been developed to be a variable exit area in the ducted fan distributed propulsion system model. The variable nozzle exit area is playing a significant role in the ducted fan distributed propulsion system model because it is one of the parameters that used to manipulate thrust and pressures throughout the flight by regulating flow through the system. The nozzle exit area is controlled by a specific PI

controller that determines the appropriate value of the nozzle exit area at each second throughout the flight profile. In other words, the nozzle exit area control system produces the variable exit area of the convergent nozzle values which are considered the output of this controller throughout the flight profile. The PI controller manipulates the values of the actual pressure ratio of the ducted fan to be equal to the desired or design pressure ratio of the aircraft design characteristics values by convergent the error to zero. Then, the values of the variable exit area of the nozzle are used to calculate the thrust of the propulsion system model despite the increase and decrease in the altitude and Mach number as well as the pressure and temperature by using Equation 34.

The graphical representation of the nozzle exit area is shown in Figure 31 below, which shows the variable exit area of the nozzle throughout the flight for one fully operational fan. Figure 32 shows the graphical representation of the nozzle variable exit area throughout the flight for one of the six back-up fans.

In Figure 31, the initial value has been chosen to be equal to 1 m^2. Also, it can be noticed that there is an abrupt increasing change in the nozzle exit area values, especially in the takeoff region.

The variable exit area starts at 1 m^2 which is the initial value at the beginning, and then the PI control system determines the variable exit area values depending on the actual and desired pressure ratio values. For example, the variable exit area values begin to increase abruptly in the takeoff to be equal to 1.14 m^2 at the highest climb point where the Mach number is 0.82 and the altitude is 32.9 Kft. Then, the values continue to increase throughout the transition and the cruise segment to reach 1.91 m^2 at the end of the cruise segment. After the cruise, the variable exit area begins to decrease in the descent to reach

1.89 m^2. Then, the values are coming back to increase slightly to be equal to 1.91-1.92 m^2 at the approach and landing.

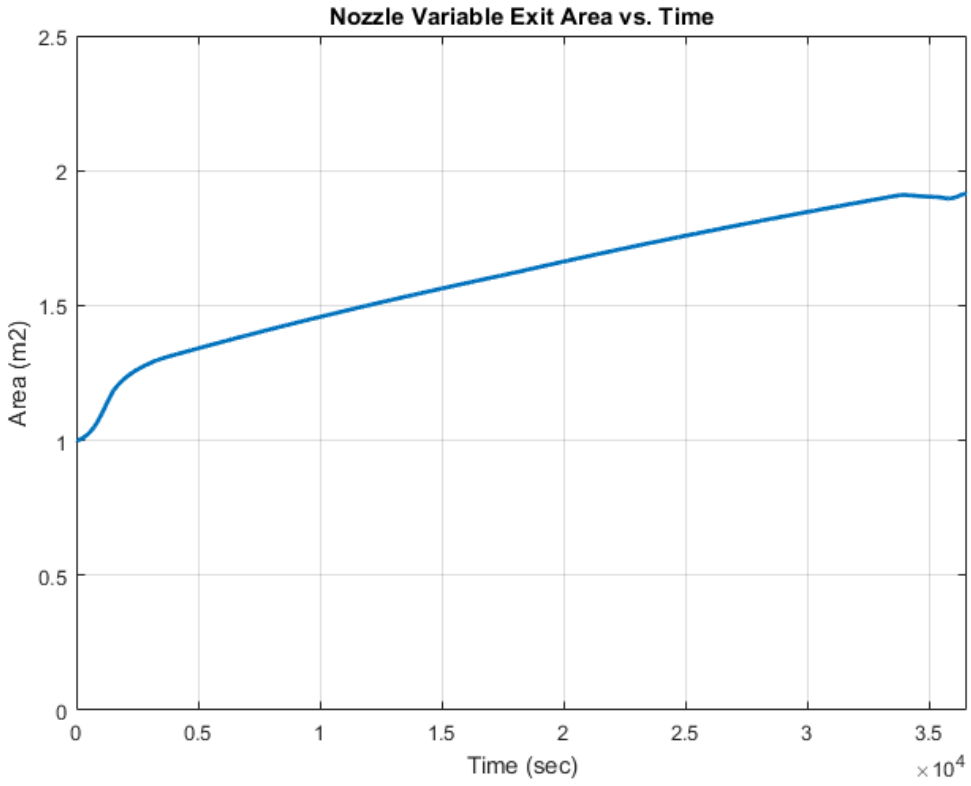

Figure 31: The Variable Exit Area of The Nozzle for One Continuous Operation Fan

There is a substantial note; the nozzle exit area is open up during the flight profile to keep the propulsion system producing the required thrust [18]. In other words, the nozzle exit area PI controller works to compensate the reduction in the pressure throughout the takeoff and cruise (i.e., when the altitude increased).

Figure 32 illustrates that the nozzle exit area plot's behavior had some similarities with the nozzle exit area plot in Figure 31. The initial value has been chosen to be equal to 1 m^2. Moreover, it can be noticed that the variable exit area values line has an abrupt increasing change in the takeoff region, approach, and landing, and there is abrupt decreasing throughout the transition area and cruise segment.

The variable exit area starts at 1 m^2 which is the initial value at the beginning, and then the PI control system generated the variable exit area values depending on the actual and desired pressure ratio values. For example, the variable exit area values begin to increase abruptly in the takeoff segment to be equal to 1.14 m^2 at the highest climb point where the Mach number is 0.82 and the altitude is 32.9 Kft. Then, the values decrease throughout the transition area, cruise, and descent segment to reach 0.4 m^2 at the end of the descent segment, where the back-up fan starts to decrease its speed to the minimum speed (i.e., it stops producing considerable thrust). After the cruise and descent segment, the values are coming back to increase slightly to be equal to 0.42-0.43 m^2 at the approach and the landing [18].

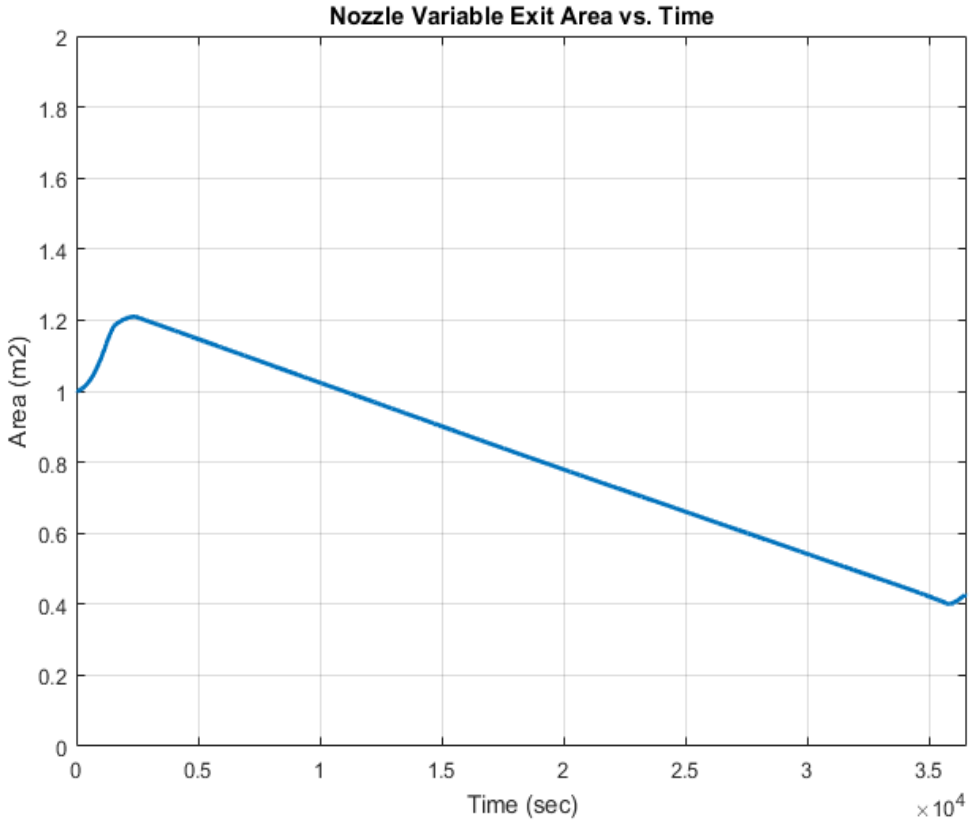

Figure 32: The Variable Exit Area of The Nozzle For One Fan of Six Back-up Fans

4.3 Boeing 777-200LR with a Notional Flight Profile

4.3.1 Flight Profile

The second case is a manuvering flight profile similar to the first case an actual flight profile of NASA N3-X except at 33 Kft altitude, 0.82 Mach number, and 123 minutes of the actual flight profile. The pilots lower the aircraft to10 Kft altitude and reduce the aircraft's speed to 0.4 Mach number for 122 minutes due to a reason such as a big storm. After that, the pilots have climbed the aircraft to complete the original flight profile, Figure 33.

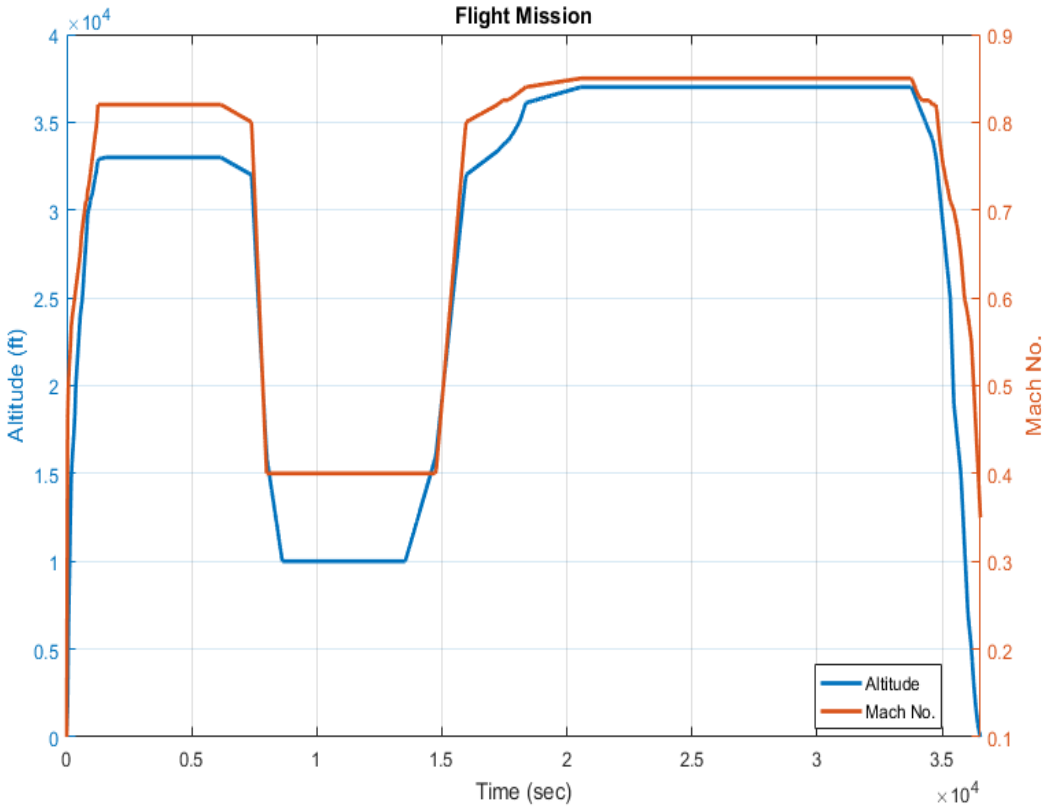

Figure 33: Second Case Notional Flight Profile

4.3.2 Thrust Actual and Thrust Demand

The thrust is considered the primary output of the ducted fan distributed propulsion system model. The thrust generated should match the thrust demanded throughout the flight. The thrust demanded values of the flight were chosen according to the NASA/Cranfield University analysis. Figure 34 below shows, the thrust generated and demanded throughout the flight for one fully operational fan. In Figure 35, one of the six back-up fan's thrust is shown.

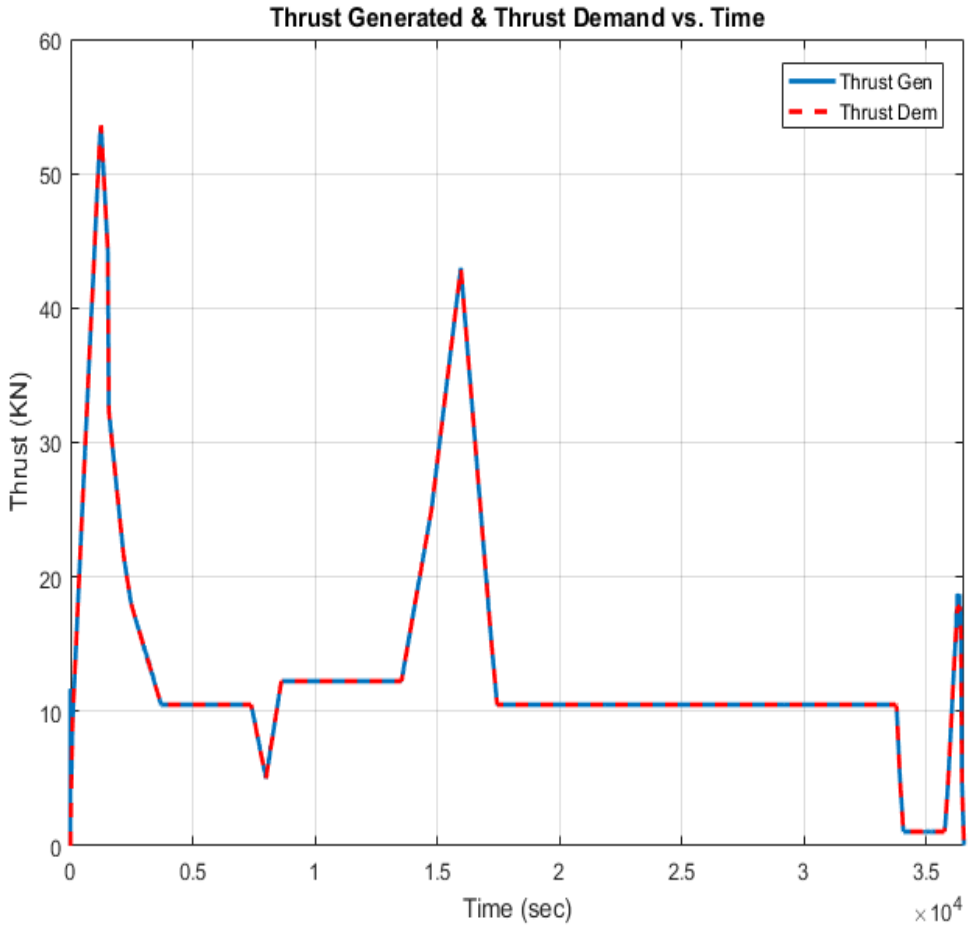

Figure 34: Second Case Thrust Generated and Demand for One Continuous Operation Fan

In Figure 34, the thrust actual is identical to the thrust demanded across the flight profile. Notice, the maximum thrust occurs through the takeoff and climb leg until the aircraft reaches the maximum altitude and starts the cruise segment. Then, the thrust values decrease in the first descent, and they increase quickly at 0.4 Mach number and 10 Kft altitude. After two hours, the thrust values increase throughout the second climb segment. The thrust value then decreases until the cruise is achieved. Next, the thrust values decrease until they reached the descent segment. Finally, the thrust values increase in the transition area until the values reach the approach and landing segment. When the approach segment ends, the thrust values decrease throughout the landing and taxi segments until the aircraft has stopped at 0 thrust.

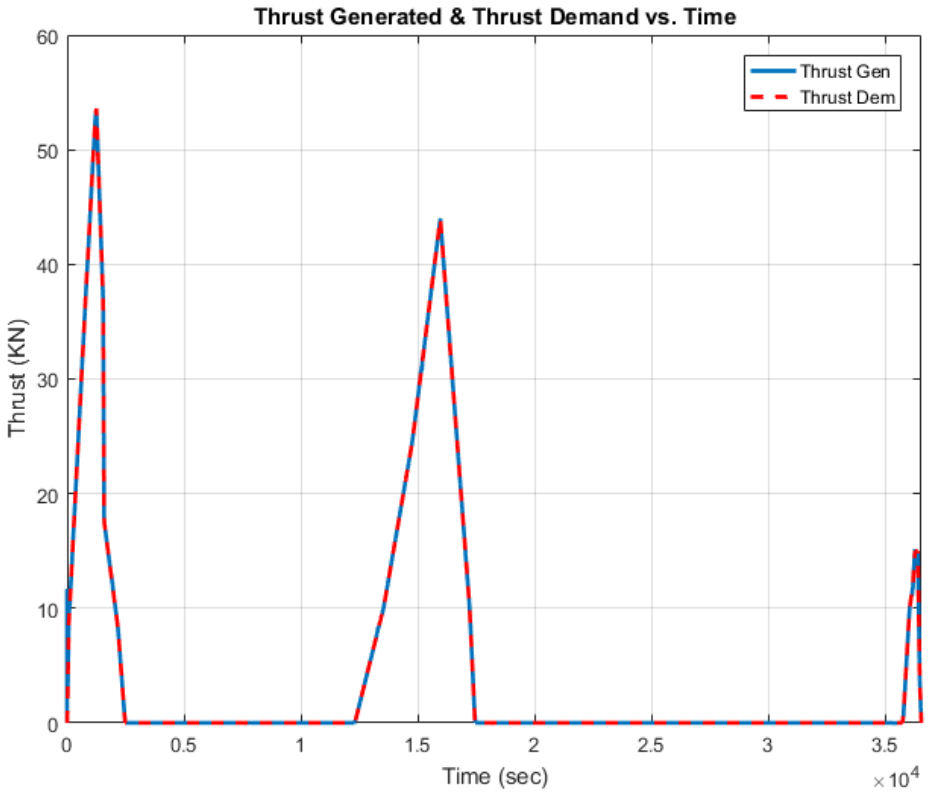

Figure 35: Second Case Thrust Generated and Demand for One Fan of Six Back-up Fans

In Figure 35, the thrust generated versus thrust demanded for the back-up fans is shown. Again, the agreement between the two thrust levels is excellent. The thrust profile clearly shows that the back-up fans are not used except for the high thrust demand segments of the flight. This performance is by design.

The thrust values start at 0 KN, and increase on the runway until reaching the maximum thrust value at takeoff. Then, the thrust begins to decrease in the transition until the thrust reaches 0 KN. After that, the thrust values increase throughout the second climb. Then, the thrust values decrease in the transition until the thrust reaches 0 KN throughout the cruise and descent segments. After the cruise and descent segments end, the thrust values began to increase until they reach the approach and landing segments. When the approach segment ends, the thrust decreases throughout the landing and taxi segments until the aircraft stops at 0 KN.

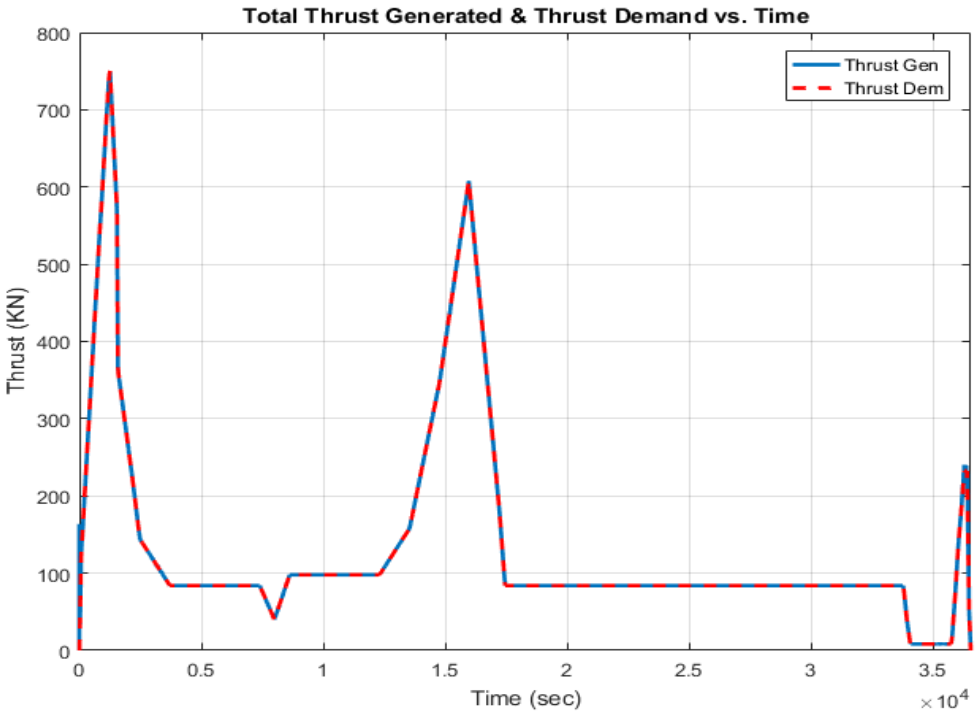

Figure 36: Second Case The Total Thrust Generated and Demand for Fourteen Fans

Figure 36 shows, the total thrust generated and thrust demanded throughout the flight. Similar to Figures 34 and 35, the agreement between the thrust generated and demanded is excellent throughout the flight.

4.3.3 Power Required

The power is considered the primary input of the ducted fan distributed propulsion system model. Figure 37 shows, the total electrical, mechanical, and dissipated power throughout the maneuvering flight for all the ducted fans.

The total electrical power starts at 0 MW and increases on the runway until reaching the maximum electrical power of 64.6 MW at takeoff. After that, the total electrical power begins to decrease until reaching the cruise segment power which is 10.2 MW. Then, the total electrical power values increase quickly until the second cruise segment electrical power of 19.8 MW is reached at 0.4 Mach number and 10 Kft altitude. After two hours, the total electrical power values increase throughout the second climbing segment electrical power of 39 MW is reached at 0.8 Mach number and 32 Kft altitude. Then, the total electrical power values decrease until the power became close to the cruise segment electrical power value. After the cruise segment ends, the total electrical power decreases until the descent electrical power of 2.3 MW is reached. Next, the total electrical power begins to increase until reaching the approach and landing segment electrical power which is 52 MW. When the approach segment ends, the electrical power begins to decrease throughout the landing and taxi segment until the aircraft stops where the electrical power is 0 MW.

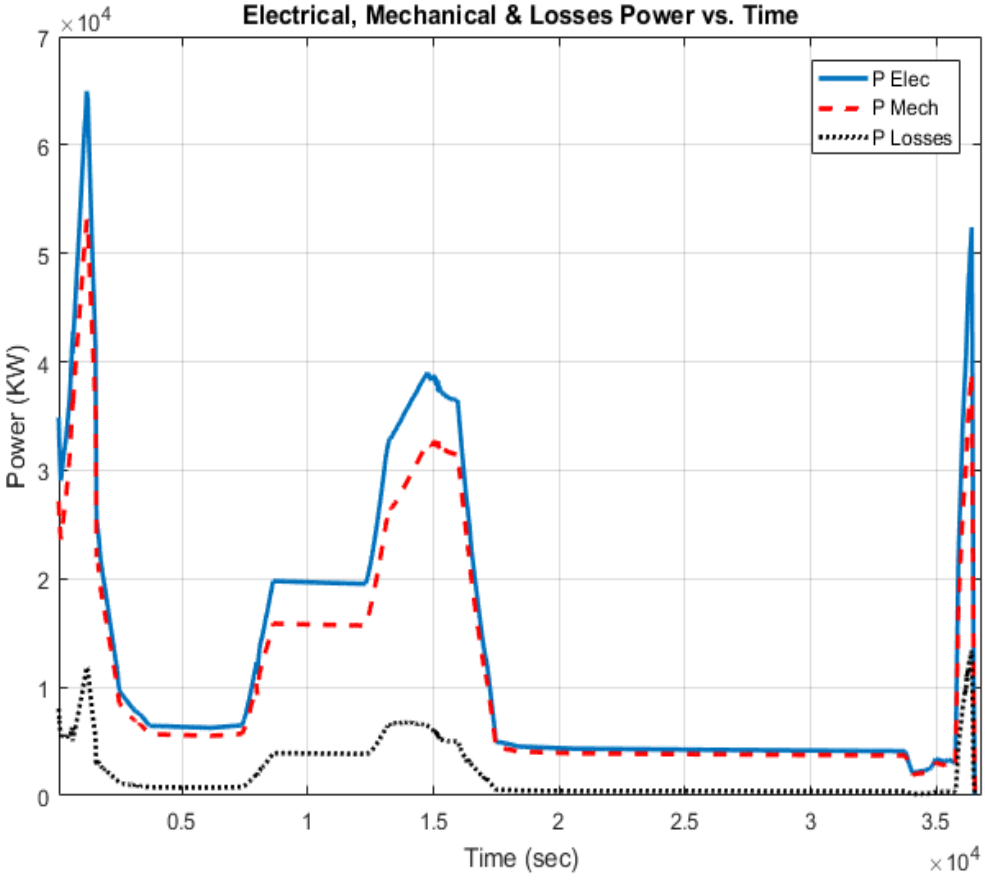

Figure 37: Second Case The Total Elec, Mech., Loss Power for Fourteen Fans

5.4 Bombardier CRJ 200 with a Notional Flight Profile

The ducted fan distributed propulsion system model of NASA N3-X aircraft is resized with the number of the passenger capacity equal to 50 passengers instead of 300 passengers for short trips (i.e., resize most of the aircraft dimensions and the total number of ducted fans and turbo-generators). As a result, Bombardier CRJ 200 aircraft is choosing to be the baseline for the resized ducted fan distributed propulsion system model of NASA N3-X aircraft. The total number of the ducted fans were chosen to be three fans with one turboelectric generator.

4.4.1 Flight Profile

The ducted fan distributed propulsion system model is used to simulate a typical regional flight profile of Bombardier CRJ 200 airplane. The CRJ 200 airplane travels from Dayton International Airport to Orlando International Airport, Figure 38. The Mach number and altitude vary throughout the flight profile.

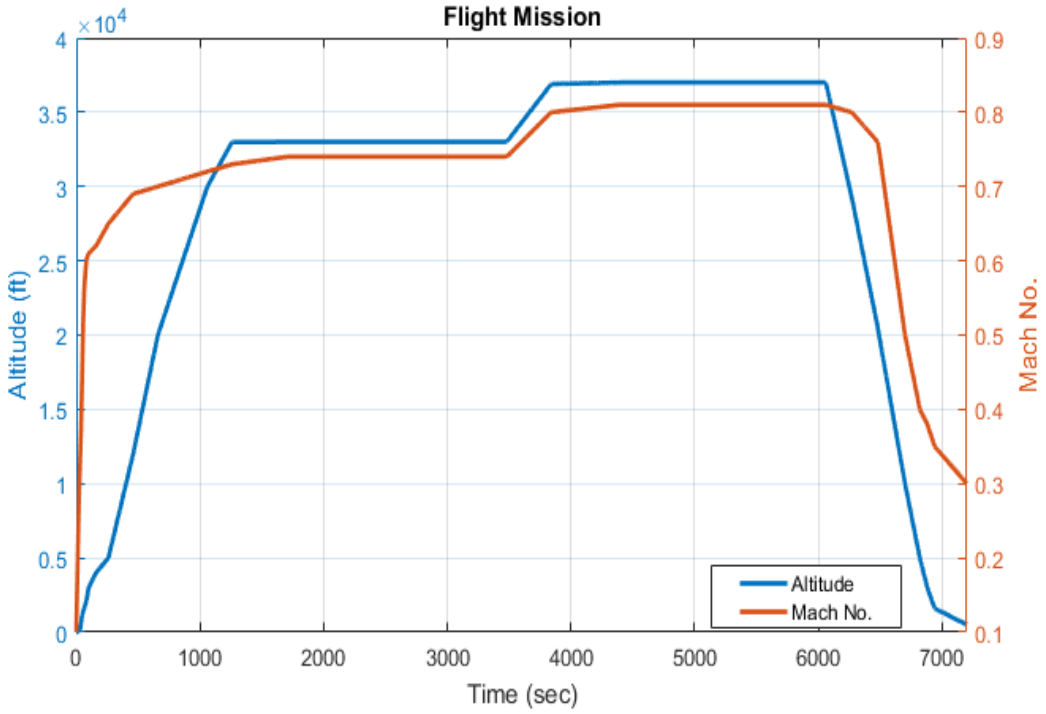

Figure 38: Third Case Resized Notional Flight Profile

The third case, a typical regional flight profile is similar to the first case, an actual flight profile except it is resized. The total simulation time of the new flight profile is 120 minutes, and the Mach number is 0.81 for a high cruise speed and 0.74 for a normal cruise speed [19].

4.4.2 Thrust Actual and Thrust Demand

The thrust is considered the major output of the ducted fan distributed propulsion system model. The thrust generated should match the thrust demanded throughout the flight. The

thrust demanded values of the flight were chosen according to the Bombardier CRJ 200 specification[19]. Figure 39 below shows, the thrust generated and demanded throughout the flight for one fully operational fan. In Figure 40, one of the six back-up fan's thrust is shown.

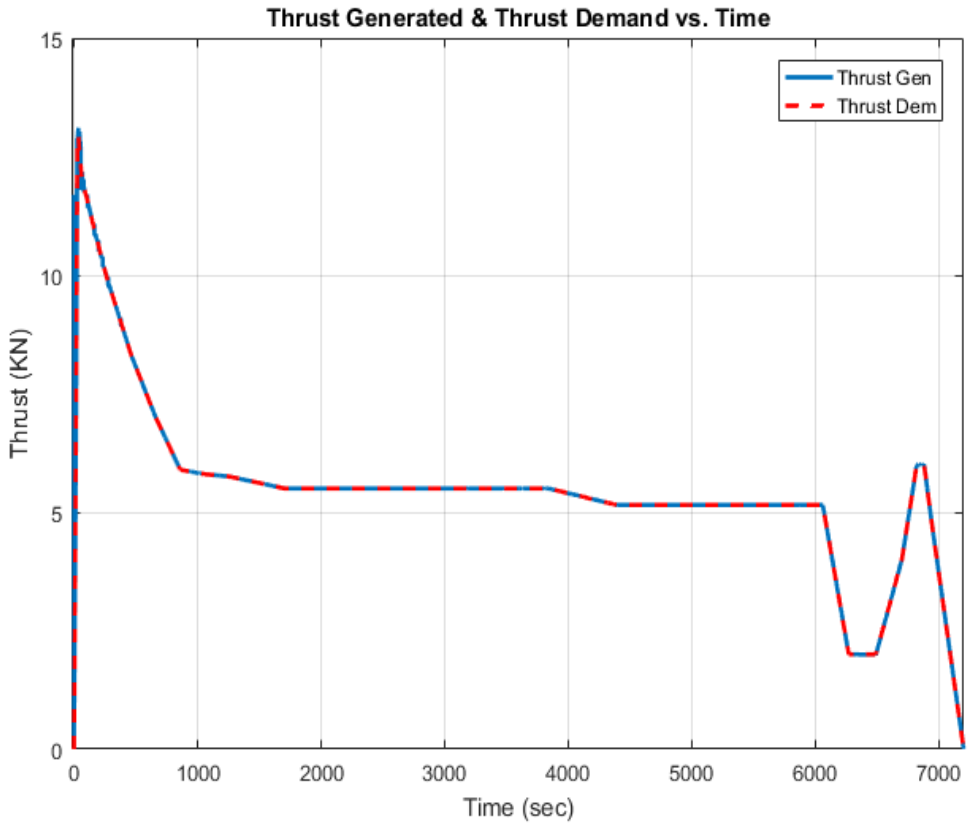

Figure 39: Third Case Thrust Generated and Demand for One Continuous Operation Fan

In Figure 39, the thrust actual is identical to the thrust demanded across the flight profile. Notice, the maximum thrust occurs through the takeoff and climb leg until the aircraft reaches the maximum altitude and starts the cruise segment. At the end of the cruise segment, the thrust values decrease until the descent. After that, the thrust values increase in the transition area until the values reached the approach and landing segment. When

the approach segment ends, the thrust values decrease throughout the landing and taxi segments until the aircraft has stopped at 0 thrust.

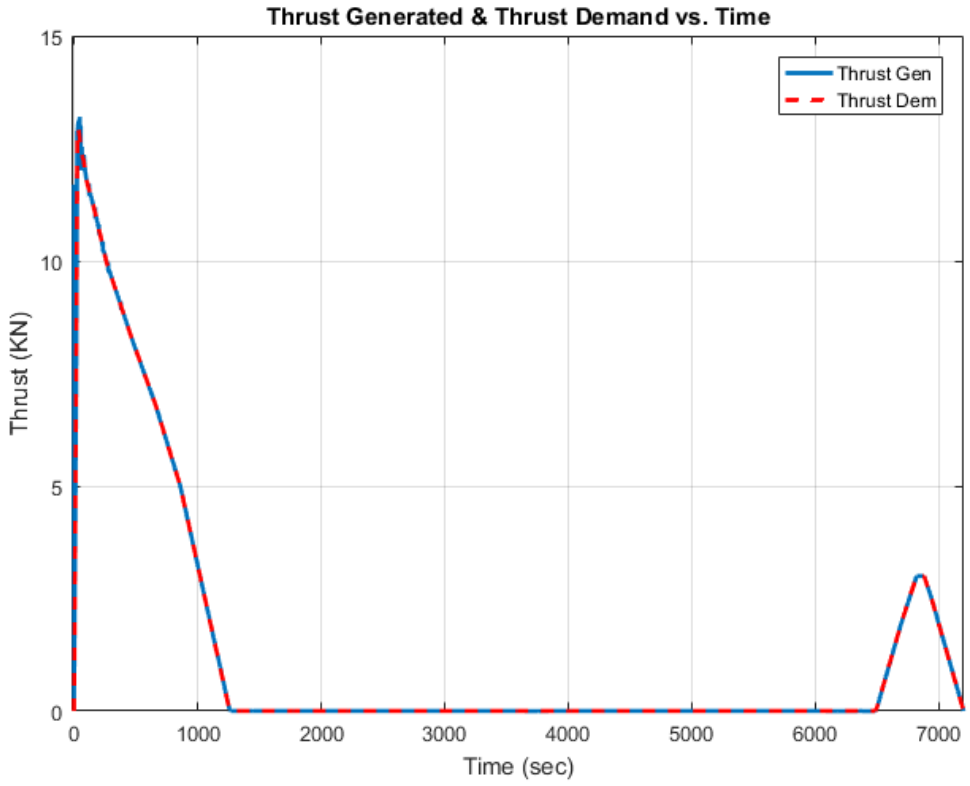

Figure 40: Third Case Thrust Generated and Demand for One Back-up Fan

In Figure 40, the thrust generated versus thrust demanded for the back-up fans is shown. Again, the agreement between the two thrust levels is excellent. The thrust profile clearly shows that the back-up fans are not used except for the high thrust demand segments of the flight. This performance is by design.

The thrust values start at 0 KN and increase on the runway until reaching the maximum thrust value at takeoff. Then the thrust begins to decrease in the transition until the thrust reaches 0 KN. After the cruise and descent segments end, the thrust values began to increase until they reached the approach and landing segment thrust . When the approach

ends, the thrust decreases throughout the landing and taxi segments until the aircraft stops at 0 KN.

Figure 41 shows, the total thrust generated and thrust demanded throughout the flight. Similar to Figures 39 and 40, the agreement between the thrust generated and demanded is excellent throughout the flight.

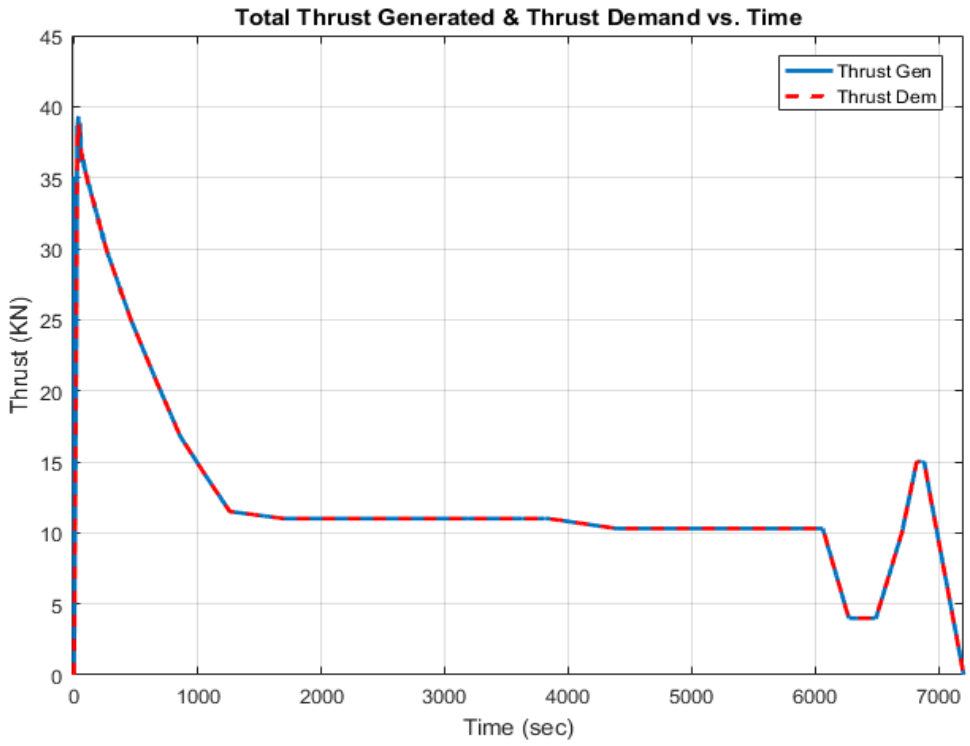

Figure 41: Second Case The Total Thrust Generated and Demand For Three Fans

4.4.3 Power Required

The power is considered the primary input of the ducted fan distributed propulsion system model. Figure 42 shows, the total electrical, mechanical, and losses power throughout the typical regional flight profile for all the ducted fans.

The total electrical power starts at 0 MW and increases on the runway until reaching the maximum electrical power of 11.4 MW at takeoff. Then, the total electrical power begins

to decrease until reaching the cruise segment power which is 1.4 MW. After the cruise segment ends, the total electrical power decreases until the descent electrical power of 0.91 MW is reached. Next, the total electrical power begins to increase until reaching the approach and landing segments electrical power which is 4.2 MW. When the approach segment ends, the electrical power begins to decrease throughout the landing and taxi-in segment until the aircraft stops where the electrical power is 0 MW.

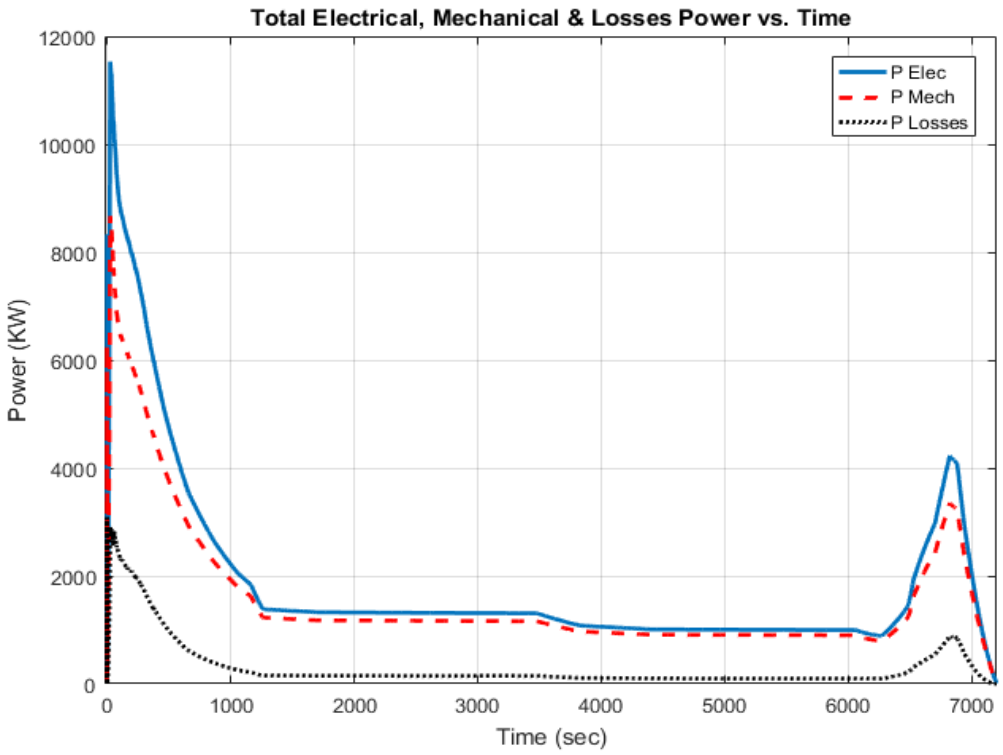

Figure 42: Third Case The Total Elec, Mech., Loss Power for Three Fans

Important notice, for all the three cases, in the transition area (climb to cruise segment) the rotational speed (rpm) of the back-up fans were reduced progressively until they rotated idly. However, in the transition area (descent to landing segment) the rotational speed (rpm) of the back-up fans were increased progressively until they reached the required speed.

5. Conclusion

The primary goals and objectives of this thesis have been achieved. A mathematical model of the Turboelectric Distributed Propulsion System (TeDP) for NASA next generation aircrafts, more specifically the N3-X aircraft, has been created and developed by using one of the numerical simulation tools called MATLAB/Simulink to achieve the assessments of the system.

In this thesis, three cases studies with the N3-X model were performed which were divided based on the aircraft baseline's type and the flight profile. The first case, the aircraft baseline's type is the Boeing 777-200LR class using NASA's defined flight. The second case, the aircraft baseline's type is the same aircraft with a maneuvering flight profile. The third case, the aircraft baseline's type is the Bombardier CRJ 200 with a typical regional flight profile.

The ducted fan distributed propulsion system model is considered a model of two ducted fans which represent the total number of the ducted fans for the three cases. For the first and second case, one of these two fans represents eight fans, and the other fan represents six back-up fans. However, for the third case; one of these two fans represent two fans, and the other fan represents one back-up fan.

For the first case, the eight fans are operating the whole flight profile, while the six fans are operating only in the takeoff and landing segment of the whole when a high thrust is needed. For the second case, the eight fans are operating the whole flight profile while

the six fans are operating in the takeoff, second climbing landing segment of the whole flight. For the third case, the two fans are operating the whole flight while the one fan is operating only in the takeoff and landing segment of the whole flight profile when a high thrust is needed.

The design FPR value of the TeDP model has been chosen to have the highest efficiency value. The FPR value was chosen depending on many factors such as the ducted fan thrust, power, diameter, drag, and efficiency, and by using hand calculation for the thrust and power at different values of the FPR.

The ducted fan distributed propulsion system model is a dynamic model and can be used for conceptual commercial and military aircrafts. More specifically, there are two different types of PI controllers for each fan that enable the model to generate the required thrust for any flight profile and thrust demand; the two different types of PI controllers are thrust controller and nozzle exit area controller.

The thrust generated by the ducted fan distributed propulsion system model is almost identical to the thrust demanded of the notional flight profile. In other words, the thrust generated has met the thrust demand reasonably well throughout the flight profile. The thrust demand values of the flight profile have been chosen according to NASA and Cranfield University.

Also, the maximum thrust needs throughout the takeoff and climb segment, and some high thrust needs throughout the approach (loiter) and landing have been achieved. Moreover, the electrical power values have been calculated in the ducted fan distributed propulsion system model depending on the required thrust values of the conceptual N3-X aircraft throughout the flight profile. In other words, the two turbo generators were

supplying the required electrical power values that had already been estimated in the propulsion system to feed the ducted fan's electrical DC motors through the transmission lines.

In the future, the Turboelectric Distributed Propulsion System model will have the capability to integrate with other MATLAB/Simulink models, such as the power generation or turboelectric generator model that supply the electrical power to TeDP model, thermal management model, and others.

In this thesis, the Turboelectric Distributed Propulsion System model is a foundation of NASA next generation aircrafts, more specifically a futuristic N3-X aircraft, for future work. However, the TeDP model presented here is functional, yet it needs improvement before it can be used for the aircrafts. For instance, the TeDP model requires a development of an advance an intelligent modern controller, such as the Linear Quadratic Regulator controller (LQR) and Fuzzy Logic Controller (FLC) in order to control the aircraft's yaw control and yaw angle by manipulating the fans speed.

6. Appendix

6.1 Fan Map Conversion

The fan performance map of the ducted fan distributed propulsion system dynamic model is modeled by using interpolation-extrapolation 2D-lookup tables. Figure 43, 44, 45, and 46 show the fan map of the model throughout the takeoff, cruise, descent, and landing segment respectively. The blue line that runs nearly horizontally represents the fan operation of the TeDP system model over the flight profile. The red line represents the surge line. The black lines that run nearly vertically represent the rotational speed line (rpm). Finally, the small red circled point represents the position on the performance map that the system is working at the end of the simulation. From the fan map plot; it can be noticed quickly that the fan model is operating below the surge line (i.e., in the safe area of the turbomachinery map).

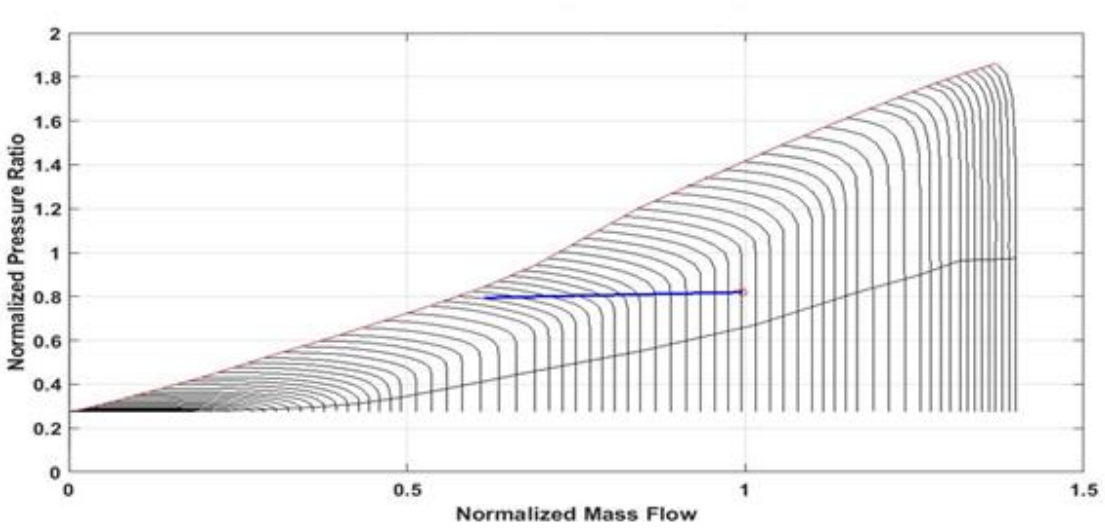

Figure 43: Fan Map of Take-Off Segment

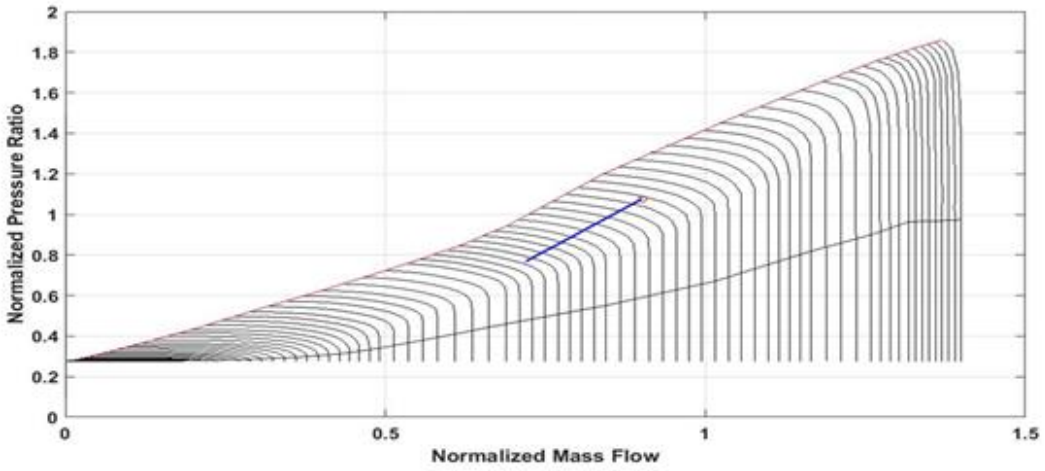

Figure 44: Fan Map of Cruise Segment

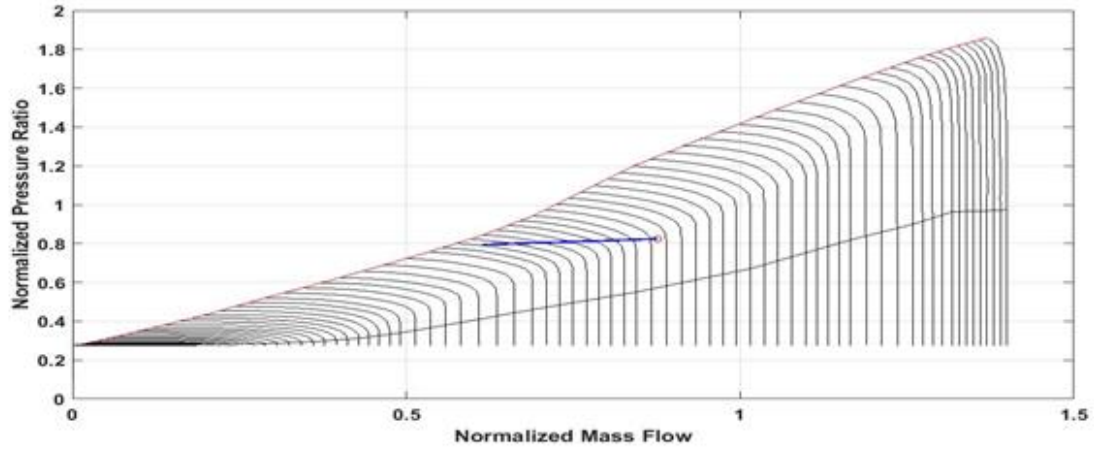

Figure 45: Fan Map of Descent Segment

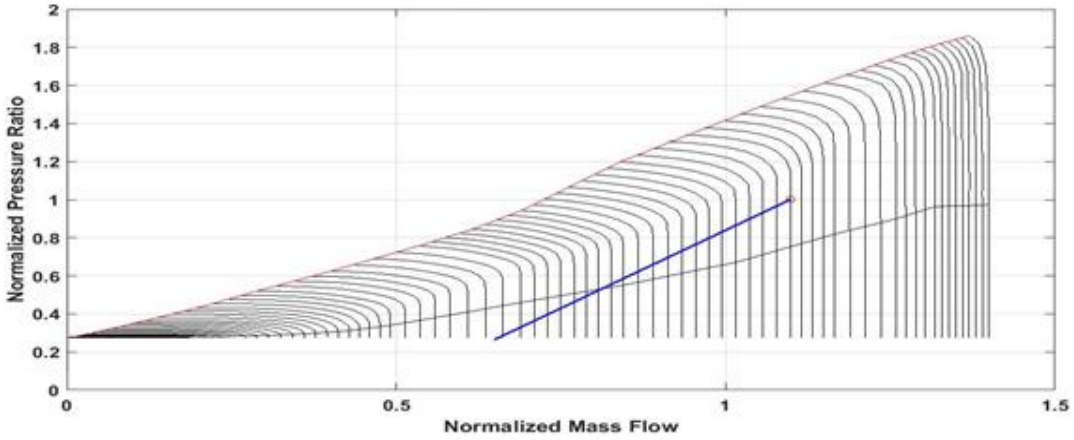

Figure 46: Fan Map of Landing Segment

REFERENCES

[1] T. Tyler, "2012 IATA Anual Review," *Director*, 2012.

[2] S. W. Ashcraft, A. S. Padron, K. A. Pascioni, G. W. Stout Jr., and D. L. Huff, "Review of Propulsion Technologies for N+3 Subsonic Vehicle Concepts," *Nasa*, no. October, pp. 1–38, 2011.

[3] J. L. Felder, "NASA N3-X with Turboelectric Distributed Propulsion," 2017.

[4] H. D. Kim, J. L. Felder, M. T. Tong, and M. J. Armstrong, "Revolutionary Aeropropulsion Concept for Sustainable Aviation: Turboelectric Distributed Propulsion," *21st Int. Symp. Air Breath. Engines*, pp. 1–12, 2013.

[5] K. Davies, P. Norman, C. Jones, S. Galloway, and M. Husband, "A review of Turboelectric Distributed Propulsion technologies for N+3 aircraft electrical systems," *Proc. Univ. Power Eng. Conf.*, 2013.

[6] C. A. Luongo *et al.*, "Next generation more-electric aircraft: a potential application for hts superconductors," *IEEE Trans. Appl. Supercond.*, vol. 19, no. 3, pp. 1055–1068, 2009.

[7] E. Giakoumakis, "Techno-economic and environmental risk assessment," 2014.

[8] J. J. Berton, E. Envia, and C. L. Burley, "An Analytical Assessment of NASA's N+1 Subsonic Fixed Wing Project Noise Goal," *15th AIAA/CEAS Aeroacoustics Conf. (30th AIAA Aeroacoustics Conf.*, no. May, pp. 11–13, 2009.

[9] H. Kim, J. Berton, and S. Jones, "Low Noise Cruise Efficient Short Take-Off and Landing Transport Vehicle Study," *6th AIAA Aviat. Technol. Integr. Oper. Conf.*, no. February, pp. 1–11, 2006.

[10] H. D. Kim, G. V. Brown, and J. L. Felder, "Distributed Turboelectric Propulsion for Hybrid Wing Body Aircraft," *2008 Int. Powered Lift Conf.*, pp. 1–11, 2008.

[11] J. L. Felder, H. D. Kim, and G. V. Brown, “Turboelectric Distributed Propulsion Engine Cycle Analysis for Hybrid-Wing-Body Aircraft,” *47th AIAA Aerosp. Sci. Meet. Incl. New Horizons Forum Aerosp. Expo.*, no. January, p. AIAA 2009-1132, 2009.

[12] R. D. Flack, *Fundamentals of Jet Propulsion with Applications*. Cambridge University Press, 2005.

[13] C. Liu, “Turboelectric Distributed Propulsion System Modelling,” 2013.

[14] S. M. Eastbourn, “Modeling and Simulation of a Dynamic Turbofan Engine Using Simulink,” 2012.

[15] O. Design, “NASA N3-X Preliminary Design Study : Final Technical Report,” vol. 3, no. May, 2016.

[16] S. Ag, “SIMOTICS FD Low-Voltage Motors Equipment for Production Machines,” *Catalog D 81.8 Edition2017*, p. 422, 2017.

[17] E. Jones, D. Doroni-dawes, and D. Larkin, “NASA N3-X Preliminary Design Study : Final Technical Report,” vol. 1, no. June, pp. 1–92, 2016.

[18] J. Mabe, “Variable Area Jet Nozzle for Noise Reduction Using Shape Memory Alloy Actuators,” *J. Acoust. Soc. Am.*, vol. 123, no. 5, pp. 5487–5492, 2008.

[19] Flight Run, “Bombardier CRJ200 Specifications,” pp. 6–8, 2012.